AN ABSTRACT OF THE THESIS OF

Mitchel Eugene Cunningham for the degree of Master of Science in Nuclear Engineering presented on May 6, 1977

Title: TEMPERATURE PROFILES OF SPHERES PACKED IN REGULAR ARRAYS

Abstract approved: Redacted for Privacy
Kenneth L. Peddicord

An analytical solution is developed for the temperature profile of a unit cell consisting of a sphere of one material centered in a cube of a second material. All material properties are considered constant and boundary conditions consist of specified temperatures on the top and bottom faces of the cube with the side faces being adiabatic. A computer program was developed using the analytical solution and results are presented. Factors of importance were found to be the ratio of the sphere diameter to the cube side length, the ratio of the thermal conductivities of the two materials, and the difference between the temperatures on the top and bottom faces of the unit cell.

Temperature Profiles of Spheres Packed in Regular Arrays

by

Mitchel Eugene Cunningham

A THESIS

submitted to

Oregon State University

in partial fulfillment of
the requirements for the
degree of

Master of Science

Commencement June 1977

APPROVED:

Redacted for Privacy

Assistant Professor of Nuclear Engineering

Redacted for Privacy

Head of Nuclear Engineering Department

Redacted for Privacy

Dean of Graduate School

Date thesis is presented May 6, 1977

Typed by Laura Collins for Mitchel Eugene Cunningham

ACKNOWLEDGMENT

I wish to express my sincere and heartfelt thanks to my advisor and friend, Dr. Kenneth L. Peddicord, for his knowledge, advice, and recommendations during the course of my graduate work.

I dedicate this thesis to my entire family; to Jeanne for encouraging me to take my Master's and helping me to find myself, to my parents and brother for their love and support, and last, but not least, to my mother-in-law for her tremendous help in the final preparation of the thesis.

TABLE OF CONTENTS

LIST OF ILLUSTRATIONS

LIST OF TABLES

TEMPERATURE PROFILE OF SPHERES PACKED IN REGULAR ARRAYS

I. Introduction

One of the engineering structures that poses a problem in heat conduction is the case of a sphere of one material surrounded by a second, differing, material. This situation may be illustrated by two examples from the field of nuclear engineering. First, the sphere has a lower thermal conductivity than the surrounding material. This may be found in ceramic fuels which contain gas pores. The gas pore may be considered as a sphere and has lower conductivity than the surrounding ceramic. Secondly, the sphere has the higher thermal conductivity. This may be illustrated by sphere packed fuel where the sphere is surrounded by a coating or by gas.

For the purpose of thermal analysis each of these examples may be approximated as consisting of a unit cell composed of a sphere centered within a regular polyhedron where the sphere is composed of one material and the remainder of the polyhedron is composed of the second material.

The first step in thermal analysis is the derivation of the temperature at any point within the chosen unit cell. This thesis will develop the analytical solution to the temperature profile of a unit cell consisting of a sphere and a regular polyhedron. Derivation of the solution will be followed by the development of a computer code based on the solution. Analysis of the code will concentrate on verifying the validity of the analytical solution, and then outlining conditions under which the code provides, or does not provide, the desired accuracy for the unit cell under consideration.

In surveying the published literature concerned with spheres and thermal analysis, it was found that there is only a limited amount of information that deals with spheres and temperature calculations. Most of the available information analyzes insulated spheres and cylinders and concentrates on finding the thermal conductance or resistance without calculating the temperatures. As an example, Schneider (1) and Yovanovich (2) have both separately investigated the thermal conductance of cylinders separating infinite planes of differing temperatures. The cylinders are assumed to be insulated except for the contact area of cylinder upon plane. Chan and Tien (3) have

extended the analysis to a packed bed of spheres separating two planes. These spheres are also considered to be insulated except for contact areas.

Holy (4) has given solutions for the subject of non-insulated spheres. He was interested in calculating the temperature and stress fields for a sphere with variable surface heat transfer and uniform internal heat generation. Using an eigenfunction expansion Holy has developed a truncated series of spherical harmonics for his solution where the coefficients of the series were obtained by application of the least squares principle to the relevant boundary conditions. A solution of the following form was generated.

$$T(\rho,\mu,\phi) = T_o(\rho) + \sum_{n=0}^{\infty}\sum_{m=0}^{n} A_{nm}\rho^n P_n^m(\mu)\cos(m\phi) + \sum_{n=1}^{\infty}\sum_{m=1}^{n} B_{nm}\rho^n P_n^m(\mu)\sin(m\phi)$$

The coefficients A_{nm} and B_{nm} are found by solving a set of simultaneous equations. Holy's solution depends on the assumption of a mean value of heat transfer from the surface of the sphere, and as such, does not require any knowledge of the surrounding material. Accuracy for this method depends on how the given points at which the heat transfer distribution is sampled are located over the surface of the sphere.

The work presented in this thesis differs from the work dealing with insulated spheres and cylinders in that the sphere under consideration here is not insulated. The work by Holy is related to the development presented here, with the following differences. First, the solutions to be developed are dependent upon the material surrounding the sphere and no assumption is made concerning the distribution of heat transfer between the sphere and the surrounding material. Secondly, the spherical harmonic coefficients will be obtained by numerical integration of the specific functions rather than using the least squares principle. And finally, a temperature profile will be developed for the entire unit cell, which includes the sphere and the surrounding material.

II. THE UNIT CELL, COORDINATE SYSTEMS, AND BOUNDARY CONDITIONS

The problem under consideration is a simple cubic, three dimensional array of spheres separating two infinite planes as shown in Figure 1a. The spheres are all of uniform diameter and consist of a homogeneous material with constant properties. The remaining volume between the two planes is occupied by a second material, also of constant properties. The array shown in Figure 1a may be reduced to a planar array as seen in Figure 1b. All boundary conditions will remain the same for the planar arrangement as for the cubic array.

The approach is an attempt to analytically describe a possible experimental arrangement. On both the upper and lower planes it will be assumed that the temperature at all points is known. For a large number of spheres in the layer, it may be concluded that no heat transfer occurs between adjacent spheres due to symmetry and that all heat transfer occurs perpendicular to the top and bottom planes.

To define the unit cell for which the study is made, the distribution of the spheres is considered. Figure 2 shows a square packed array of spheres as viewed from

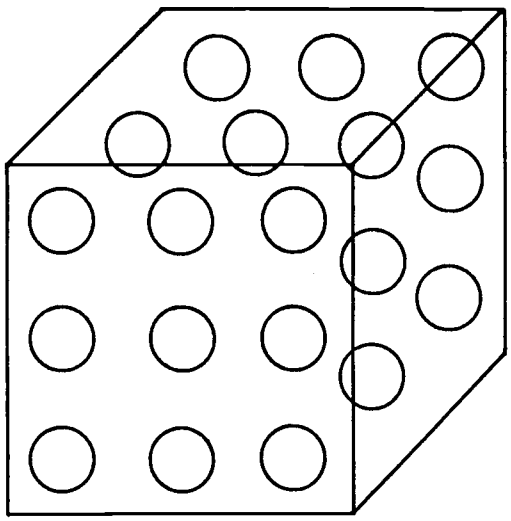

a) Simple cubic packing arrangement of spheres

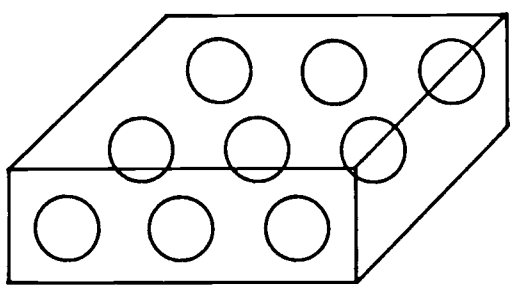

b) Repeating horizontal planes of spheres

Figure 1: Three dimensional array of spheres

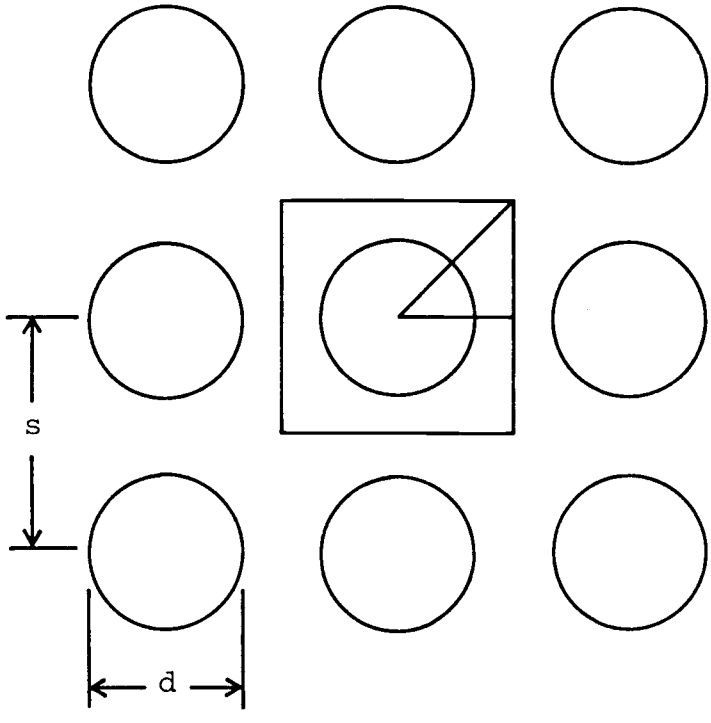

Figure 2: Central sphere in a square array with the cubical boundary and the unit cell outlined

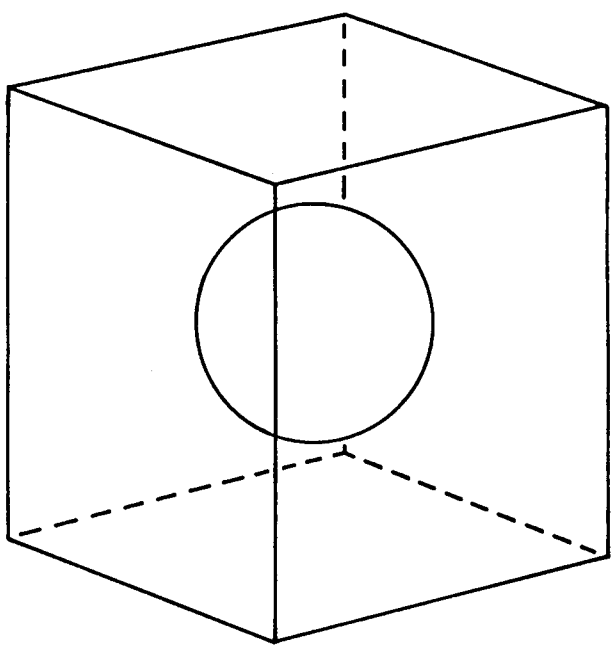

Figure 3: Single sphere centered within a cube

either the top or bottom plane. As shown in Figure 2, the analysis to be presented here will be based on an array of spheres spaced on a regular square lattice, but the diameter (d) of the spheres may be less than, or equal to, the spacing of the lattice (s). For any particular case which is to be analyzed, the diameter of all spheres will be equal and constant for that case.

The square that has been placed around the central sphere in Figure 2 defines the boundaries of a cube surrounding the sphere, with the sphere centered in the cube. Figure 3 shows a three-dimensional view of the sphere within the cube. These cubes may be replicated to construct the three-dimensional array of spheres between two planes as shown in Figure 1.

The cube and sphere can be subdivided further. In Figure 3 the temperature profiles are assumed known, and differing, on both the top and bottom faces, therefore, the full height of the cube must be considered. However, in the other directions lines of symmetry do exist. Since the heat will be flowing between the top and bottom faces due to their temperature difference, and because all sphere containing cubes are identical, no heat will be transferred across the side faces of a cube to adjacent cubes. These

side faces are therefore seen to be adiabatic. Referring again to Figure 2, it is seen that the top face can be subdivided into eight 45° right triangles by drawing lines from the center of the sphere to the corners of the square and from the center of the sphere to the midpoint of each side. These lines establish lines of symmetry; that is, the derivative of the temperature along each of these lines is zero since the temperature profiles within the cube and sphere will be either maxima or minima along these lines. Finally then the smallest unit cell which can represent the array of spheres is shown in Figure 4. It is a triangular wedge of height $2R_c$. The sides forming the right angle are each of length R_c and the hypotenuse is of length $R_c \sqrt{2}$. It is for this unit cell that the study is made.

Three plane views of the unit cell are shown in Figure 5. The top face of the triangular wedge with the outer edge of the sphere appears in Figure 5a. In Figures 5b and 5c, two of the sides of the unit cell are shown. In Figure 5b it is seen that $2R_c$ is the length of the side of the cube and that R_s is the radius of the sphere. When comparing R_c to R_s, it may be seen that R_c can be considered as the cube "radius" and will be referred to as such from here on.

This problem is treated in spherical geometry.

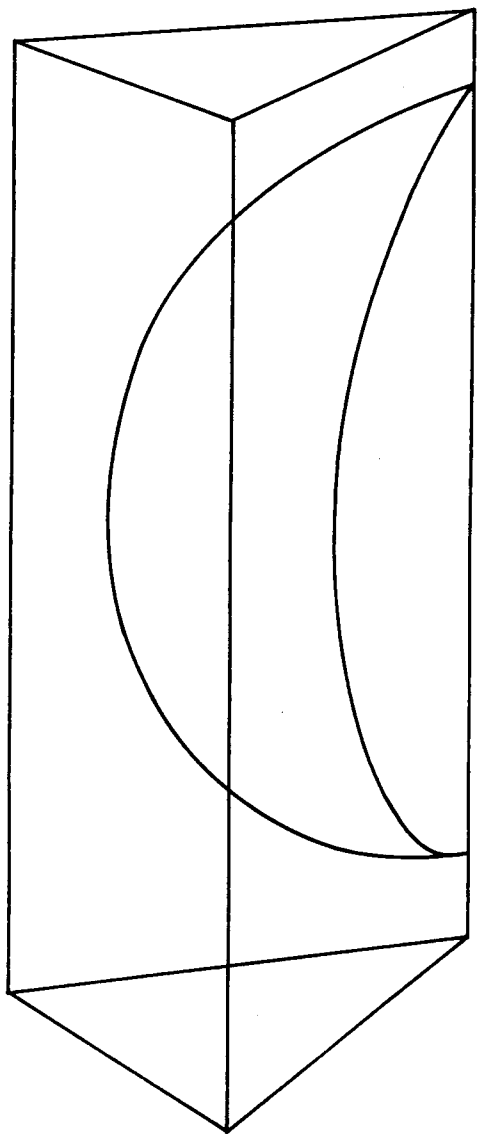

Figure 4: The unit cell for the square array

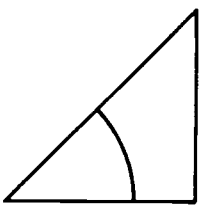

a) Top view, $Z = R_C$

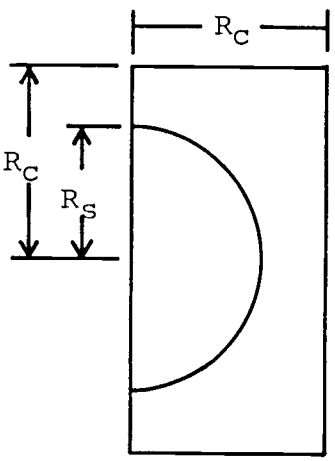

b) Side view, $Y = 0$, $\phi = 0$

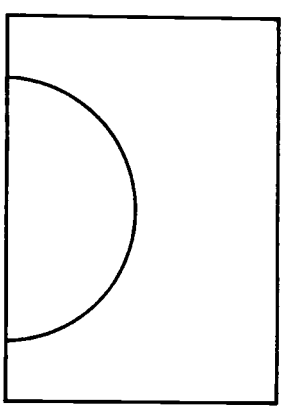

c) Side view, $X = Y$, $\phi = \pi/4$

Figure 5: Three views of the unit cell

Figure 6 is a repeat of Figure 4, but has the spherical and cartesian coordinate systems imposed upon it. Any point P in the unit cell is described by the coordinates (ρ,α,ϕ) where ρ is the distance from the origin to P, α is the angle between the Z axis and the line to P, and ϕ is the angle between the X axis and the projection of the line to P on the XY plane.

Steady state heat conduction in this spherical system is governed by Poisson's equation:

$$\nabla^2\theta(\rho,\alpha,\phi) = 0 \qquad \text{(II-1)}$$

where $\theta(\rho,\alpha,\phi)$ is the temperature at any point within the unit cell. The Laplacian operator is given by

$$\nabla^2 = \frac{1}{\rho^2}\frac{\partial}{\partial\rho}\left(\rho^2\frac{\partial}{\partial\rho}\right) + \frac{1}{\rho^2\sin\alpha}\frac{\partial}{\partial\alpha}\left(\sin\alpha\frac{\partial}{\partial\alpha}\right) + \frac{1}{\rho^2\sin^2\alpha}\frac{\partial^2}{\partial\phi^2} \qquad \text{(II-2)}$$

A more useful form can be obtained by making the transformation

$$\mu = \cos\alpha \qquad (1-\mu^2)^{1/2} = \sin\alpha \qquad \text{(II-3)}$$

so that

$$\nabla^2 = \frac{1}{\rho^2}\frac{\partial}{\partial\rho}\left(\rho^2\frac{\partial}{\partial\rho}\right) + \frac{1}{\rho^2}\frac{\partial}{\partial\mu}\left((1-\mu^2)\frac{\partial}{\partial\mu}\right) + \frac{1}{\rho^2(1-\mu^2)}\frac{\partial^2}{\partial\phi^2} \qquad \text{(II-4)}$$

Referring to Figure 6, the unit cell is bounded by the limits of $\phi = 0$ to $\phi = \pi/4$, $\alpha = 0$ to $\alpha = \pi$ ($\mu = 1$ to $\mu = -1$), and from $\rho = 0$ to the outer planes, top, side,

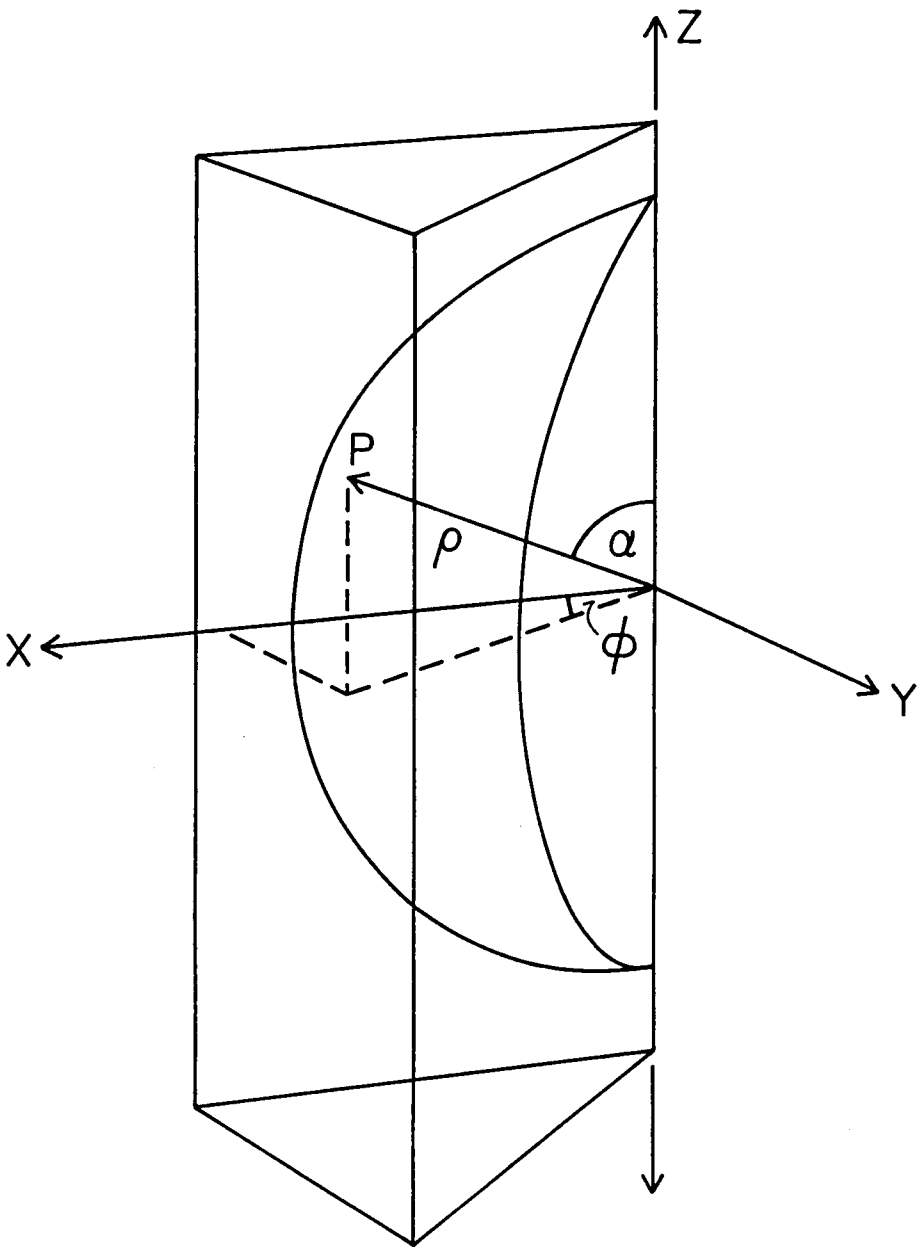

Figure 6: Coordinate systems imposed on the unit cell

and bottom, which are given by the equations in Appendix C.

There are five surfaces to the unit cell. The top and bottom faces are discussed below. The three side faces (referring to Figure 6) are: (1) the Y = 0 plane ($\phi = 0$), (2) the 45° plane given by X = Y ($\phi = \pi/4$) and (3) the plane given by $X = R_c$ (see Appendix C). These three surfaces are adiabatic. This condition requires that the component of the heat flux vector normal to the surface be zero;

$$\hat{n}_i \cdot \vec{q}''(\rho,\alpha,\phi)\Big|_{S_i} = 0 \qquad \text{(II-5)}$$

where S_i denotes the i^{th} surface, $\hat{n}_i$ is the unit vector normal to surface i, and $\vec{q}''$ is the heat flux vector.

Equation (II-5) requires that the dot product of the unit vector normal to the i^{th} surface and the heat flux vector evaluated on the i^{th} surface be zero. The heat flux vector at any point is given by

$$\vec{q}''(\rho,\alpha,\phi) = -K\vec{\nabla}\theta(\rho,\alpha,\phi) \qquad \text{(II-6)}$$

where $\vec{\nabla}$, the gradient operator, is given by

$$\vec{\nabla} = \hat{e}_\rho \frac{\partial}{\partial\rho} + \hat{e}_\alpha \frac{1}{\rho}\frac{\partial}{\partial\alpha} + \hat{e}_\phi \frac{1}{\rho\sin\alpha}\frac{\partial}{\partial\phi} \qquad \text{(II-7)}$$

where $\hat{e}_\rho$, $\hat{e}_\alpha$ and $\hat{e}_\phi$ are the unit vectors in the ρ, α and ϕ directions. Equation (III-5) may now be written as:

$$-n_i \cdot K\vec{\nabla}\theta(\rho,\alpha,\phi)\Big|_{S_i} = 0 \qquad \text{(II-8)}$$

On the top face, $Z = R_c$, the temperature at any point on the plane is known and given by the function $\theta_T(\mu,\phi)$. Likewise on the bottom face, $Z = -R_c$, the temperature at any point on the plane is known and given by the function $\theta_B(\mu,\phi)$. K is the thermal conductivity of the region under consideration.

III. DEVELOPMENT OF THE SOLUTIONS

A) General Solution of the Differential Equation

The governing equations are a linear system of ordinary differential equations. The normal procedure for solving a system of this type is used; that is, the general solution is obtained by determining the complete solution of the homogeneous equation and one particular solution to the inhomogeneous equation. The linear combination of these gives the general solution. The arbitrary coefficients in the solutions to the homogeneous equation are then evaluated through application of the boundary conditions.

The development of the solution for the temperature profile is begun by setting

$$\nabla^2\theta = 0$$

where ∇^2 is given by equation (II-4), thus giving

$$0 = \frac{1}{\rho^2}\frac{\partial}{\partial\rho}\left(\rho^2\frac{\partial\Theta}{\partial\rho}\right) + \frac{1}{\rho^2}\frac{\partial}{\partial\mu}\left((1-\mu^2)\frac{\partial\Theta}{\partial\mu}\right) + \frac{1}{\rho^2}\frac{1}{(1-\mu^2)}\frac{\partial^2\Theta}{\partial\phi^2} \qquad \text{(III-1)}$$

It becomes advantageous at this point to convert to non-dimensional parameters and proceed with the analysis upon that basis. Distance and temperature are the two parameters affected and the non-dimensional terms are

defined by:

$$r = \frac{\rho}{R_c} \qquad T = \frac{\theta(\rho,\mu,\phi) - \theta_B(\mu,\phi)}{\theta_T(\mu,\phi) - \theta_B(\mu,\phi)}$$

where θ_T and θ_B are the temperature functions on the top and bottom faces of the unit cell. Equation (III-1) is now converted by substituting in the appropriate expressions for ρ, θ, and $\frac{\partial}{\partial \rho}$.

$$\rho = rR_c$$

$$\theta = T(\theta_T - \theta_B) + \theta_B$$

$$\frac{\partial}{\partial \rho} = \frac{\partial r}{\partial \rho}\frac{\partial}{\partial r} = \frac{1}{R_c}\frac{\partial}{\partial r}$$

Thus giving:

$$0 = \frac{1}{r^2 R_c^2}\frac{1}{R_c}\left(r^2 R_c^2 \frac{\partial}{\partial r}\left(T(\theta_T - \theta_B) + \theta_B\right)\right)$$
$$+ \frac{1}{r^2 R_c^2}\frac{\partial}{\partial \mu}\left((1-\mu^2)\frac{\partial}{\partial \mu}\left(T(\theta_T - \theta_B) + \theta_B\right)\right)$$
$$+ \frac{1}{r^2 R_c^2}\frac{1}{(1-\mu^2)}\frac{\partial^2}{\partial \phi^2}\left(T(\theta_T - \theta_B) + \theta_B\right)$$

Now combining terms and performing the partial derivatives upon $T(\theta_T - \theta_B) + \theta_B$ produces:

$$0 = \frac{(\theta_T - \theta_B)}{R_c^2}\frac{1}{r^2}\frac{\partial}{\partial r}\left(r^2 \frac{\partial T}{\partial r}\right) + \frac{(\theta_T - \theta_B)}{R_c^2}\frac{1}{r^2}\frac{\partial}{\partial \mu}\left((1-\mu^2)\frac{\partial T}{\partial \mu}\right)$$
$$+ \frac{(\theta_T - \theta_B)}{R_c^2}\frac{1}{r^2(1-\mu^2)}\frac{\partial^2 T}{\partial \phi^2}$$

Dividing through by the constant factor gives the following final form:

$$0 = \frac{1}{r^2}\frac{\partial}{\partial r}\left(r^2\frac{\partial T}{\partial r}\right) + \frac{1}{r^2}\frac{\partial}{\partial \mu}\left((1-\mu^2)\frac{\partial T}{\partial \mu}\right) + \frac{1}{r^2(1-\mu^2)}\frac{\partial^2 T}{\partial \phi^2} \qquad \text{(III-2)}$$

The solution to equation (III-2) may be represented by eigenfunctions of the form

$$T(r,\mu,\phi) = E(r)F(\mu)G(\phi)$$

To identify the specific functions, it becomes necessary to examine the operators.

If $G(\phi)$ is selected as $\cos(k\phi)$, it is seen that two derivatives return the cosine function. One of the boundary conditions applicable to this problem is that

$$\left.\frac{\partial T(r,\mu,\phi)}{\partial \phi}\right|_{\phi=\frac{\pi}{4}} = 0$$

This is due to the symmetry of the unit cell. Application of the boundary condition leads to the conclusion that

$$-k\sin(k\phi) = 0$$

Knowing that $\sin(\pi) = 0$, this sets up the condition that $k\phi = \pi$. When $\phi = \pi/4$, then k must equal 4. To make the solution hold for all multiples of π, $k = 4m$, where m is an integer greater than, or equal to, zero. Therefore it is seen that all modes of the form

$$G(\phi) = \cos(4m\phi)$$

satisfy the equation.

It is also desired that when E(r) is operated upon by the Laplacian, that the original function be returned. One function which satisfies this requirement is

$$E(r) = r^n$$

Another function which satisfies this requirement is

$$E(r) = r^{-n-1}$$

This second form of E(r) will be of importance later. The following form has now been established for the temperature solution:

$$T(r,\mu,\phi) = r^n F(\mu)\cos(4m\phi)$$

To determine a specific function for $F(\mu)$, it becomes necessary to evaluate the partial derivatives of $T(r,\mu,\phi)$ with respect to r and ϕ, and then insert those expressions into the governing equation, equation (III-2).

$$\frac{\partial T(r,\mu,\phi)}{\partial r} = n r^{n-1} F(\mu)\cos(4m\phi)$$

$$\frac{1}{r^2}\frac{\partial}{\partial r}\left(r^2 \frac{\partial T(r,\mu,\phi)}{\partial r}\right) = n(n+1) r^{n-2} F(\mu)\cos(4m\phi)$$

$$\frac{\partial T(r,\mu,\phi)}{\partial \phi} = -4m r^n F(\mu)\sin(4m\phi)$$

$$\frac{\partial^2 (T(r,\mu,\phi))}{\partial \phi^2} = -(4m)^2 r^n F(\mu)\cos(4m\phi)$$

Combining these partial derivatives gives the following equation.

$$0 = n(n+1)r^{n-2}F(\mu)\cos(4m\phi) + \frac{1}{r^2}\frac{\partial}{\partial\mu}\left[(1-\mu^2)\frac{\partial}{\partial\mu}\left(r^n F(\mu)\cos(4m\phi)\right)\right] + \frac{1}{r^2(1-\mu^2)}\left[-(4m)^2 r^n F(\mu)\cos(4m\phi)\right]$$

Dividing through by r^{n-2} and $\cos(4m\phi)$ gives

$$0 = n(n+1)F(\mu) + \frac{\partial}{\partial\mu}\left[(1-\mu^2)\frac{\partial F(\mu)}{\partial\mu}\right] - \frac{(4m)^2}{(1-\mu^2)}F(\mu)$$

Further rearrangement gives an equation of the form

$$0 = \frac{\partial}{\partial\mu}\left[(1-\mu^2)\frac{\partial F(\mu)}{\partial\mu}\right] + \left[n(n+1) - \frac{(4m)^2}{(1-\mu^2)}\right]F(\mu) \qquad \text{(III-3)}$$

Equation (III-3) is the governing equation for $F(\mu)$, solving for $F(\mu)$ will complete the solution for $T(r,\mu,\phi)$. From Abramowitz and Stegun (5), equation 8.1.1, it is found by inspection that

$$F(\mu) = P_n^{4m}(\mu) + Q_n^{4m}(\mu) \qquad \text{(III-4)}$$

where $P_n^{4m}(\mu)$ and $Q_n^{4m}(\mu)$ are the associated Legendre functions of degree n and order 4m. Equation (III-4) is the total solution for $F(\mu)$ as $P_n^{4m}(\mu)$ and $Q_n^{4m}(\mu)$ are the two linearly independent solutions that satisfy the second order differential equation (III-3). Because $Q_n^{4m}(\mu)$ is

infinite at $\mu = 0$, $Q_n^{4m}(\mu)$ must be discarded and the final solution for $F(\mu)$ will be

$$F(\mu) = P_n^{4m}(\mu)$$

The final general form of $T(r,\mu,\phi)$ is now

$$T(r,\mu,\phi) = r^n P_n^{4m}(\mu)\cos(4m\phi) \qquad \text{(III-5)}$$

Now knowing the general form of the temperature solution, it becomes possible to solve for the specific temperature within the sphere and outside of the sphere.

Within the sphere:

$$\nabla^2 T_1(r,\mu,\phi) = 0$$

and outside the sphere:

$$\nabla^2 T_2(r,\mu,\phi) = 0$$

The following solutions may then be seen to satisfy the governing equations and the condition of finite temperatures at all points within the unit cell.

$$T_1(r,\mu,\phi) = C_{oo}^{(1)} + \sum_{n=1}^{\infty}\sum_{m=0}^{(n/4)} C_{nm}^{(1)} r^n P_n^{4m}(\mu)\cos(4m\phi) \qquad \text{(III-6)}$$

The r^{-n-1} term is infinite at $r = 0$ and is therefore discarded in the temperature solution for the sphere.

$$T_2(r,\mu,\phi) = C_{oo}^{(2)} + \frac{C_{oo}^{(3)}}{r} + \sum_{n=1}^{\infty}\sum_{m=0}^{(n/4)}\left(C_{nm}^{(2)} r^n + C_{nm}^{(3)} r^{-n-1}\right) P_n^{4m}(\mu)\cos(4m\phi) \qquad \text{(III-7)}$$

Where (n/4) denotes the largest integer in n/4 and $C_{oo}^{(1)}$, $C_{oo}^{(2)}$, $C_{oo}^{(3)}$, $C_{nm}^{(1)}$, $C_{nm}^{(2)}$, and $C_{nm}^{(3)}$ are all constants which

must be evaluated.

B) Detailed Treatment and Application of the Boundary Conditions.

The boundary conditions which are applicable to this problem and will be used to solve for the constants in the temperature solutions are:

1) Continuity of temperature, for all μ and ϕ, at the interface between the sphere and the remainder of the unit cell.
2) Continuity of heat flux, for all μ and ϕ, at the interface between the sphere and the remainder of the unit cell.
3) The $\phi = 0$ and $\phi = \pi/4$ faces of the unit cell are adiabatic. (This condition was used to select the $\cos(4m\phi)$ mode.)
4) The outer faces of the cube are subject to one boundary condition, which consists of three parts:
    a) The top face of the unit cell has a known temperature function, $\theta_T(\mu,\phi)$
    b) The outer side face of the unit cell is

adiabatic. (This face will be referred to as the side face of the unit cell.)

c) The bottom face of the unit cell has a known temperature function, $\theta_B(\mu,\phi)$

Boundary conditions 1) and 2) will each provide two equations for the solution of the constants.

Continuity of temperature requires that $T_1(R_a,\mu,\phi) = T_2(R_a,\mu,\phi)$ must be satisfied at $r = R_s/R_c = R_a$.

$$C_{oo}^{(1)} + \sum_{n=1}^{\infty}\sum_{m=0}^{(n/4)} C_{nm}^{(1)} R_a^n P_n^{4m}(\mu)\cos(4m\phi) = C_{oo}^{(2)} + \frac{C_{oo}^{(3)}}{R_a} + \sum_{n=1}^{\infty}\sum_{m=0}^{(n/4)} \left(C_{nm}^{(2)} R_a^n + C_{nm}^{(3)} R_a^{-n-1} \right) P_n^{4m}(\mu)\cos(4m\phi) \qquad \text{(III-8)}$$

It is now possible to operate on equation (III-8) and utilize the orthogonal properties of the cosine function. This is done by operating on both sides of the equation by $\int_0^{\pi/4} \cos(4k\phi)\,d\phi$. This is done twice, first with $k = 0$, and secondly for all other k.

With $k = 0$, the involved portion of the equation is

$$\int_0^{\pi/4} \cos(4m\phi)\,d\phi = \frac{1}{4m}\sin(4m\phi)\Big|_0^{\pi/4} = 0$$

and

$$\int_0^{\pi/4} d\phi = \frac{\pi}{4}$$

This then gives

$$\frac{\pi}{4}\left[C_{00}^{(1)}\right] + 0\left[\sum_{n=1}^{\infty}\sum_{m=0}^{(n/4)} C_{nm}^{(1)} R_a^n P_n^{4m}(\mu)\cos(4m\phi)\right] = \frac{\pi}{4}\left[C_{00}^{(2)} + \frac{C_{00}^{(3)}}{R_a}\right]$$

$$+ 0\left[\sum_{n=1}^{\infty}\sum_{m=0}^{(n/4)} \left(C_{nm}^{(2)} R_a^n + C_{nm}^{(3)} R_a^{-n-1}\right) P_n^{4m}(\mu)\cos(4m\phi)\right]$$

which has a final form of

$$C_{00}^{(1)} = C_{00}^{(2)} + \frac{C_{00}^{(3)}}{R_a} \qquad \text{(III-9)}$$

Now applying orthogonality for all $k>0$,

$$\int_0^{\pi/4} \cos(4m\phi)\cos(4k\phi)\, d\phi$$

requires a change of variable. Setting $w = 4\phi$, this then gives

$$\frac{1}{4}\int_{w=0}^{w=\pi} \cos(mw)\cos(kw)\, dw = \begin{cases} \frac{\pi}{8} & , \ k = m \\ 0 & , \ k \neq m \end{cases}$$

Applying this to equation (III-8) then produces

$$\frac{\pi}{8}\sum_{n=1}^{\infty} C_{nk}^{(1)} R_a^n P_n^{4k}(\mu) = \frac{\pi}{8}\sum_{n=1}^{\infty}\left(C_{nk}^{(2)} R_a^n + C_{nk}^{(3)} R_a^{-n-1}\right) P_n^{4k}(\mu) \qquad \text{(III-10)}$$

The next step utilizes the orthogonality of the associated Legendre functions. This is done by operating on equation (III-10) with

$$\int_{-1}^{1} P_l^{4k}(\mu)\, d\mu$$

Noting that from Abramowitz and Stegun (5), equation 8.14.13

$$\int_{-1}^{1} P_n^{4k}(\mu)\, P_\ell^{4k}(\mu)\, d\mu = \begin{cases} \dfrac{2}{2\ell+1}\,\dfrac{(\ell+4k)!}{(\ell-4k)!} & , k \le \dfrac{\ell}{4} \ , \ \ell = n \\ 0 & , k \le \dfrac{\ell}{4} \ , \ \ell \neq n \end{cases}$$

This gives the result of

$$\frac{\pi}{8}\,\frac{2}{2\ell+1}\,\frac{(\ell+4k)!}{(\ell-4k)!}\,C_{\ell k}^{(1)}\,R_a^{\ell}$$

$$= \frac{\pi}{8}\,\frac{2}{2\ell+1}\,\frac{(\ell+4k)!}{(\ell-4k)!}\left(C_{\ell k}^{(2)}\,R_a^{\ell} + C_{\ell k}^{(3)}\,R_a^{-\ell-1}\right)$$

The above equation may be reduced to the following system of linear equations

$$C_{\ell k}^{(1)}\,R_a^{\ell} = C_{\ell k}^{(2)}\,R_a^{\ell} + C_{\ell k}^{(3)}\,R_a^{-\ell-1} \qquad \text{(III-11)}$$

The second boundary condition to be applied is that of continuity of heat flux, normal to the surface of the sphere, at $r = R_a$, that is

$$-K_1 \frac{\partial}{\partial r}\, T_1(R_a, \mu, \phi) = -K_2 \frac{\partial}{\partial r}\, T_2(R_a, \mu, \phi)$$

$$K_1 \sum_{n=1}^{\infty} \sum_{m=0}^{(n/4)} n\, C_{nm}^{(1)}\, R_a^{n-1}\, P_n^{4m}(\mu)\cos(4m\phi) = K_2 \left\{ \frac{C_{00}^{(3)}}{R_a^2} + \sum_{n=1}^{\infty} \sum_{m=0}^{(n/4)} \left(n\, C_{nm}^{(2)}\, R_a^{-n-1} - (n+1)\, C_{nm}^{(3)}\, R_a^{-n-2} \right) P_n^{4m}(\mu)\cos(4m\phi) \right\} \qquad \text{(III-12)}$$

Using orthogonality as before, we first operate with

$$\int_0^{\pi/4} d\phi$$ which gives

$$0 = \frac{\pi}{4} K_2 \frac{C_{oo}^{(3)}}{R_a^2}$$

which uniquely defines $C_{oo}^{(3)}$ as

$$C_{oo}^{(3)} = 0 \qquad \text{(III-13)}$$

and reduces equation (III-9) to

$$C_{oo}^{(1)} = C_{oo}^{(2)} \qquad \text{(III-14)}$$

The next step is to operate on equation (III-12) with

$$\int_0^{\pi/4} \cos(4k\phi)\, d\phi \quad .$$ This gives

$$\frac{\pi}{8} K_1 \sum_{n=0}^{\infty} n C_{nk}^{(1)} R_a^{n-1} P_n^{4k}(\mu) = \frac{\pi}{8} K_2 \sum_{n=1}^{\infty} \left(C_{nk}^{(2)} R_a^{n-1} - (n+1) C_{nk}^{(3)} R_a^{-n-2} \right) P_n^{4k}(\mu)$$

Now operating on the result with $\int_{-1}^{1} P_\ell^{4k}(\mu)\, d\mu$

the following result is obtained

$$\frac{\pi}{8} \frac{2}{2\ell+1} \frac{(\ell+4k)!}{(\ell-4k)!} K_1 \ell C_{\ell k}^{(1)} R_a^{\ell-1} = \frac{\pi}{8} \frac{2}{2\ell+1} \frac{(\ell+4k)!}{(\ell-4k)!}$$

$$\cdot K_2 \left(\ell C_{\ell k}^{(2)} R_a^{\ell-1} - (\ell+1) C_{\ell k}^{(3)} R_a^{-\ell-2} \right)$$

which may be reduced to the following system of linear equations.

$$K_1 \ell C_{\ell k}^{(1)} R_a^{\ell-1} = K_2 \left(\ell C_{\ell k}^{(2)} R_a^{\ell-1} - (\ell+1) C_{\ell k}^{(3)} R_a^{-\ell-2} \right) \qquad \text{(III-15)}$$

There is now one equation, (III-14), for the two unknown coefficients $C_{oo}^{(1)}$ and $C_{oo}^{(2)}$, and two equations, (III-11) and (III-15) for the unknown coefficients $C_{1k}{}^{(1)}$ and $C_{1k}{}^{(2)}$, and $C_{1k}{}^{(3)}$. It now becomes necessary to obtain one more equation for $C_{1k}{}^{(1)}$, $C_{1k}{}^{(2)}$ and $C_{1k}{}^{(3)}$ so that their solution may be obtained. This will be accomplished by applying the boundary condition to the outer faces of the unit cell.

Beginning with the top face of the unit cell, the boundary condition of known temperature function may be written as

$$\theta(\rho,\mu,\phi) = \theta_T(\mu,\phi)$$

and this may be rewritten as

$$T_2(r,\mu,\phi) = 1$$

Therefore

$$1 = C_{oo}^{(2)} + \sum_{n=1}^{\infty}\sum_{m=0}^{(n/4)}\left(C_{nm}^{(2)} r^n + C_{nm}^{(3)} r^{-n-1}\right) P_n^{4m}(\mu)\cos(4m\phi)$$

The boundary condition equation may be written in the following form so that it will be easier to use later.

$$1 = C_{oo}^{(2)} + \sum_{n=1}^{\infty}\sum_{m=0}^{(n/4)}\Big[C_{nm}^{(2)} r^n P_n^{4m}(\mu)\cos(4m\phi) + C_{nm}^{(3)} r^{-n-1} P_n^{4m}(\mu)\cos(4m\phi)\Big]$$

From Appendix C, it is shown that the top face is defined by the following relations

$$r = \frac{1}{\mu} \quad , \quad \frac{1}{(2+\tan^2\phi)^{1/2}} \leq \mu \leq 1 \quad , \quad 0 \leq \phi \leq \frac{\pi}{4}$$

Now substituting in the expression for r, the final form of the equation is obtained.

$$1 = C_{oo}^{(2)} + \sum_{n=1}^{\infty} \sum_{m=0}^{(n/4)} \left[C_{nm}^{(2)} \left(\frac{1}{\mu}\right)^n P_n^{4m}(\mu) \cos(4m\phi) + C_{nm}^{(3)} \left(\frac{1}{\mu}\right)^{-n-1} P_n^{4m}(\mu) \cos(4m\phi) \right] \quad \text{(III-16)}$$

Equation (III-16) may be rewritten in the following general form

$$1 = C_{oo}^{(2)} + \sum_{n=1}^{\infty} \sum_{m=0}^{(n/4)} \left[C_{nm}^{(2)} F_{nm}^{(1)}(\mu) \cos(4m\phi) + C_{nm}^{(3)} G_{nm}^{(1)}(\mu) \cos(4m\phi) \right] \quad \text{(III-17)}$$

where

$$F_{nm}^{(1)}(\mu) = \left(\frac{1}{\mu}\right)^n P_n^{4m}(\mu)$$

$$G_{nm}^{(1)}(\mu) = \left(\frac{1}{\mu}\right)^{-n-1} P_n^{4m}(\mu)$$

The next face to be evaluated is the side face, $X = R_c$, where

$$r = \frac{1}{\cos\phi\,(1-\mu^2)^{1/2}} \qquad \text{(See Appendix C)}$$

The boundary condition here is that the face is adiabatic,

that is, no heat transfer occurs across the face. The unit vector normal to the side face is $\hat{n} = \hat{e}_x$. The boundary condition for this face may then be written as

$$\hat{e}_x \cdot \vec{q} = \hat{e}_x \cdot \left[-K_2 \vec{\nabla} T_2(r,\mu,\phi) \right] = 0 \qquad \text{(III-18)}$$

where $\vec{q}$ is the heat flux, $\hat{e}_x \cdot \vec{q}$ is the component perpendicular to the side face and $\vec{\nabla} T_2(r,\mu,\phi)$ is again defined as

$$\vec{\nabla} T_2(r,\mu,\phi) = \hat{e}_r \frac{\partial T_2(r,\mu,\phi)}{\partial r} + \hat{e}_\alpha \frac{1}{r} \frac{\partial T_2(r,\mu,\phi)}{\partial \alpha} + \hat{e}_\phi \frac{1}{r \sin\alpha} \frac{\partial T_2(r,\mu,\phi)}{\partial \alpha}$$

Utilizing the transformations for spherical unit vectors in terms of the cartesian unit vectors (see Appendix A), it is seen that the dot products in equation (III-18) become

$$\hat{e}_x \cdot \hat{e}_r = \sin\alpha\cos\phi$$

$$\hat{e}_x \cdot \hat{e}_\alpha = \cos\alpha\cos\phi$$

$$\hat{e}_x \cdot \hat{e}_\phi = -\sin\phi$$

so that

$$\hat{e}_x \cdot \vec{q} = -K_2 \left[\sin\alpha\cos\phi \frac{\partial T_2(r,\mu,\phi)}{\partial r} + \frac{\cos\alpha\cos\phi}{r} \frac{\partial T_2(r,\mu,\phi)}{\partial \alpha} - \frac{\sin\phi}{r\sin\alpha} \frac{\partial T_2(r,\mu,\phi)}{\partial \phi} \right] \qquad \text{(III-19)}$$

The next step is to evaluate the three partial derivatives. Recalling that

$$T_2(r,\mu,\phi) = C_{00}^{(2)} + \sum_{n=1}^{\infty}\sum_{m=0}^{(n/4)}\left(C_{nm}^{(2)} r^n + C_{nm}^{(3)} r^{-n-1}\right) P_n^{4m}(\mu)\cos(4m\phi)$$

and that $\mu = \cos\alpha$, the three derivatives are seen to be:

$$\frac{\partial T_2(r,\mu,\phi)}{\partial r} = \sum_{n=1}^{\infty}\sum_{m=0}^{(n/4)}\left(nC_{nm}^{(2)} r^{n-1} - (n+1) r^{-n-2}\right) P_n^{4m}(\mu)\cos(4m\phi)$$

$$\frac{\partial T_2(r,\mu,\phi)}{\partial \phi} = -\sum_{n=1}^{\infty}\sum_{m=0}^{(n/4)}\left(C_{nm}^{(2)} r^n + C_{nm}^{(3)} r^{-n-1}\right) P_n^{4m}(\mu)\, 4m \sin(4m\phi)$$

$$\frac{\partial T_2(r,\mu,\phi)}{\partial \alpha} = \sum_{n=1}^{\infty}\sum_{m=0}^{(n/4)}\left(C_{nm}^{(2)} r^n + C_{nm}^{(3)} r^{-n-1}\right) \frac{\partial}{\partial\alpha}\left(P_n^{4m}(\mu)\right)\cos(4m\phi)$$

Realizing that

$$\frac{\partial}{\partial\alpha} P_n^{4m}(\mu) = \frac{\partial\mu}{\partial\alpha}\frac{\partial}{\partial\mu} P_n^{4m}(\mu)$$

and

$$\frac{d\mu}{d\alpha} = \frac{d\cos\alpha}{d\alpha} = -\sin\alpha = -(1-\mu^2)^{1/2}$$

The next step is to solve for $\frac{\partial}{\partial\mu}P_n^{4m}(\mu)$. This is done by making use of equation 8.5.4 of Abramowitz and Stegun (5) which states (in their notation)

$$(z^2-1)\frac{d}{dz} P_\nu^\mu(z) = \nu z\, P_\nu^\mu(z) - (\nu+\mu) P_{\nu-1}^\mu(z)$$

It is then seen for the problem under consideration that

$$\frac{d}{d\mu} P_n^{4m}(\mu) = \frac{n\mu P_n^{4m}(\mu) - (n+4m) P_{n-1}^{4m}(\mu)}{\mu^2 - 1}$$

The parts may now be put together to show that

$$\frac{\partial}{\partial \alpha} P_n^{4m}(\mu) = -(1-\mu^2)^{1/2} \left\{ \frac{n\mu P_n^{4m}(\mu) - (n+4m) P_{n-1}^{4m}(\mu)}{\mu^2 - 1} \right\}$$

which may be rewritten as

$$\frac{\partial}{\partial \alpha} P_n^{4m}(\mu) = \frac{n\mu P_n^{4m}(\mu) - (n+4m) P_{n-1}^{4m}(\mu)}{(1-\mu^2)^{1/2}}$$

It is now seen that

$$\frac{\partial T_2(r,\mu,\phi)}{\partial \alpha} = \sum_{n=1}^{\infty} \sum_{m=0}^{(n/4)} \left(C_{nm}^{(2)} r^n + C_{nm}^{(3)} r^{-n-1} \right) \cdot \left(\frac{n\mu P_n^{4m}(\mu) - (n+4m) P_{n-1}^{4m}(\mu)}{(1-\mu^2)^{1/2}} \right) \cos(4m\phi)$$

It is now necessary to insert all three partial derivatives into equation (III-18) to solve the boundary condition.

This then yields the following expression

$$0 = \left\{ (1-\mu^2)^{1/2} \cos\phi \sum_{n=1}^{\infty} \sum_{m=0}^{(n/4)} \left(n C_{nm}^{(2)} r^{n-1} - (n+1) C_{nm}^{(3)} r^{-n-2} \right) P_n^{4m}(\mu) \cos(4m\phi) \right.$$

$$+ \frac{\mu \cos\phi}{r} \sum_{n=1}^{\infty} \sum_{m=0}^{(n/4)} \left(C_{nm}^{(2)} r^n + C_{nm}^{(3)} r^{-n-1} \right) \left(\frac{n\mu P_n^{4m}(\mu) - (n+4m) P_{n-1}^{4m}(\mu)}{(1-\mu^2)^{1/2}} \right) \cos(4m\phi)$$

$$\left. + \frac{\sin\phi}{r(1-\mu^2)^{1/2}} \sum_{n=1}^{\infty} \sum_{m=0}^{(n/4)} \left(C_{nm}^{(2)} r^n + C_{nm}^{(3)} r^{-n-1} \right) P_n^{4m}(\mu) \sin(4m\phi) \right\} \quad \text{(III-20)}$$

Equation (III-19) has already been divided by $-K_2$ and the expressions $\sin\alpha = (1-\mu^2)^{1/2}$ and $\cos\alpha = \mu$ have been in-

serted. Now bringing the constants inside the summations

$$0 = \sum_{n=1}^{\infty}\sum_{m=0}^{(n/4)}\left(nC_{nm}^{(2)}r^{n-1} - (n+1)C_{nm}^{(3)}r^{-n-2}\right)P_n^{4m}(\mu)(1-\mu^2)^{1/2}\cos(4m\phi)\cos\phi$$

$$+\sum_{n=1}^{\infty}\sum_{m=0}^{(n/4)}\left(C_{nm}^{(2)}r^{n-1} + C_{nm}^{(3)}r^{-n-2}\right)\left(\frac{n\mu^2 P_n^{4m}(\mu) - (n+4m)\mu P_{n-1}^{4m}(\mu)}{(1-\mu^2)^{1/2}}\right)\cos(4m\phi)\cos\phi$$

$$+\sum_{n=1}^{\infty}\sum_{m=0}^{(n/4)}\left(C_{nm}^{(2)}r^{n-1} + C_{nm}^{(3)}r^{-n-2}\right)\frac{P_n^{4m}(\mu)}{(1-\mu^2)^{1/2}}\sin(4m\phi)\sin\phi$$

Now combining all three summations

$$0 = \sum_{n=1}^{\infty}\sum_{m=0}^{(n/4)}\left\{C_{nm}^{(2)}r^{n-1}\left(nP_n^{4m}(\mu)(1-\mu^2)^{1/2}\cos(4m\phi)\cos\phi\right.\right.$$

$$+\left(\frac{n\mu^2 P_n^{4m}(\mu) - (n+4m)\mu P_{n-1}^{4m}(\mu)}{(1-\mu^2)^{1/2}}\right)\cos(4m\phi)\cos\phi$$

$$\left.+\frac{P_n^{4m}(\mu)}{(1-\mu^2)^{1/2}}\sin(4m\phi)\sin\phi\right) + C_{nm}^{(3)}r^{-n-2}\left(-(n+1)P_n^{4m}(\mu)(1-\mu^2)^{1/2}\right.$$

$$\cdot\cos(4m\phi)\cos\phi + \left(\frac{n\mu^2 P_n^{4m}(\mu) - (n+4m)\mu P_{n-1}^{4m}(\mu)}{(1-\mu^2)^{1/2}}\right)\cos(4m\phi)\cos\phi$$

$$\left.\left.+\frac{P_n^{4m}(\mu)}{(1-\mu^2)^{1/2}}\sin(4m\phi)\sin\phi\right)\right\}$$

Substituting in $r = \dfrac{1}{\cos\phi\,(1-\mu^2)^{1/2}}$ and further simplifying

$$0 = \sum_{n=1}^{\infty}\sum_{m=0}^{(n/4)}\left\{\frac{C_{nm}^{(2)}}{\cos^{n-1}\phi(1-\mu^2)^{\frac{n-1}{2}}}\left[\left(n(1-\mu^2)^{1/2}P_n^{4m}(\mu) + \frac{n\mu^2 P_n^{4m}(\mu) - (n+4m)\mu P_{n-1}^{4m}(\mu)}{(1-\mu^2)^{1/2}}\right)\right.\right.$$

$$\cdot\cos(4m\phi)\cos\phi + \left.\frac{4mP_n^{4m}(\mu)}{(1-\mu^2)^{1/2}}\sin(4m\phi)\sin\phi\right] + \frac{C_{nm}^{(3)}}{\cos^{-n-2}\phi\,(1-\mu^2)^{\frac{-n-2}{2}}}$$

$$\cdot\left[\left(\frac{n\mu^2 P_n^{4m}(\mu) - (n+4m)\mu P_{n-1}^{4m}(\mu)}{(1-\mu^2)^{1/2}} - (n+1)(1-\mu^2)^{1/2}P_n^{4m}(\mu)\right)\cos(4m\phi)\cos\phi\right.$$

$$\left.\left.+\frac{4mP_n^{4m}(\mu)}{(1-\mu^2)^{1/2}}\sin(4m\phi)\sin\phi\right]\right\}$$

By combining $P_n^{4m}(\mu)$ terms and separating out $(1-\mu^2)^{1/2}$ the above equation may be simplified to the following intermediate form.

$$0=\sum_{n=1}^{\infty}\sum_{m=0}^{(n/4)}\left\{\frac{C_{nm}^{(2)}}{\cos^{n-1}\phi\,(1-\mu^2)^{\frac{n-1}{2}}}\left[\left(nP_n^{4m}(\mu)-(n+4m)\mu P_{n-1}^{4m}(\mu)\right)\frac{\cos(4m\phi)\cos\phi}{(1-\mu^2)^{1/2}}\right.\right.$$

$$\left.+\frac{4m\,P_n^{4m}(\mu)}{(1-\mu^2)^{1/2}}\sin(4m\phi)\sin\phi\right]+\frac{C_{nm}^{(3)}}{\cos^{-n-2}\phi\,(1-\mu^2)^{\frac{-n-2}{2}}}\left[\left(\left(\mu^2(2n+1)-(n+1)\right)\right.\right.$$

$$\left.\left.\cdot P_n^{4m}(\mu)-(n+4m)\mu P_{n-1}^{4m}(\mu)\right)+\frac{4m\,P_n^{4m}(\mu)}{(1-\mu^2)^{1/2}}\sin(4m\phi)\sin\phi\right]\Bigg\}$$

A final simplification by combining $(1-\mu^2)^{1/2}$ yields

$$0=\sum_{n=1}^{\infty}\sum_{m=0}^{(n/4)}\left\{\frac{C_{nm}^{(2)}}{\cos^{n-1}\phi\,(1-\mu^2)^{n/2}}\left[\left(nP_n^{4m}(\mu)-(n+4m)\mu P_{n-1}^{4m}(\mu)\right)\cos(4m\phi)\cos\phi\right.\right.$$

$$\left.+4m\,P_n^{4m}(\mu)\sin(4m\phi)\sin\phi\right]+\frac{C_{nm}^{(3)}}{\cos^{-n-2}\phi\,(1-\mu^2)^{\frac{-n-1}{2}}}\left[\left(\left(\mu^2(2n+1)-(n+1)\right)\right.\right.$$

$$\left.\left.\cdot P_n^{4m}(\mu)-(n+4m)\mu P_{n-1}^{4m}(\mu)\right)\cos(4m\phi)\cos\phi+4m\,P_n^{4m}(\mu)\right.$$

$$\left.\cdot\sin(4m\phi)\sin\phi\right]\Bigg\} \qquad \text{(III-21)}$$

Equation (III-21) may now be written in the same form used for the top face.

$$0=\sum_{n=1}^{\infty}\sum_{m=0}^{(n/4)}\left[C_{nm}^{(2)}\left(F_{nm}^{(2)}(\mu)\cos(4m\phi)\cos\phi+F_{nm}^{(3)}(\mu)\sin(4m\phi)\sin\phi\right)\right.$$

$$\left.+C_{nm}^{(3)}\left(G_{nm}^{(2)}(\mu)\cos(4m\phi)\cos\phi+G_{nm}^{(3)}(\mu)\sin(4m\phi)\sin\phi\right)\right] \qquad \text{(III-22)}$$

where

$$F_{nm}^{(2)}(\mu) = \frac{1}{\cos^{n-1}\phi\,(1-\mu^2)^{n/2}}\left(n P_n^{4m}(\mu) - (n+4m)\mu P_{n-1}^{4m}(\mu)\right)$$

$$F_{nm}^{(3)}(\mu) = \frac{1}{\cos^{n-1}\phi\,(1-\mu^2)^{n/2}}\left(4m P_n^{4m}(\mu)\right)$$

$$G_{nm}^{(2)}(\mu) = \frac{1}{\cos^{-n-2}\phi\,(1-\mu^2)^{\frac{-n-1}{2}}}\left((\mu^2(2n+1)-(n+1))P_n^{4m}(\mu) - (n+4m)\mu P_{n-1}^{4m}(\mu)\right)$$

$$G_{nm}^{(3)}(\mu) = \frac{1}{\cos^{-n-2}\phi\,(1-\mu^2)^{\frac{-n-1}{2}}}\left(4m P_n^{4m}(\mu)\right)$$

Equation (III-22) is valid for the side face of the unit cell under the following conditions.

$$r = \frac{1}{\cos\phi\,(1-\mu^2)^{1/2}}$$

$$-\frac{1}{(2+\tan^2\phi)^{1/2}} \le \mu \le \frac{1}{(2+\tan^2\phi)^{1/2}}$$

$$0 \le \phi \le \frac{\pi}{4}$$ (See Appendix B)

The final face to be evaluated is the bottom face of the unit cell where the boundary condition is that the temperature distribution across the face is a known function. The equation of the bottom face is

$$r = \frac{-1}{\mu}$$

and the boundary condition may be stated as

$$\theta(\rho,\mu,\phi) = \theta_B(\mu,\phi)$$

which may be rewritten as

$$T_2(r,\mu,\phi) = 0$$

The boundary equation is now seen to be

$$0 = C_{oo}^{(2)} + \sum_{n=1}^{\infty} \sum_{m=0}^{(n/4)} \left(C_{nm}^{(2)} r^{n} + C_{nm}^{(3)} r^{-n-1} \right) P_n^{4m}(\mu) \cos(4m\phi) \qquad \text{(III-23)}$$

After substituting in $r = \frac{-1}{\mu}$ and further rearrangement, equation (III-23) may be written in final form as

$$0 = C_{oo}^{(2)} + \sum_{n=1}^{\infty} \sum_{m=0}^{(n/4)} \left[C_{nm}^{(2)} \left(\frac{-1}{\mu} \right)^{n} P_n^{4m}(\mu) \cos(4m\phi) + C_{nm}^{(3)} \left(-\frac{1}{\mu} \right)^{-n-1} P_n^{4m}(\mu) \cos(4m\phi) \right] \qquad \text{(III-24)}$$

Equation (III-24) is seen to have the same general form that has already been found for the top and side faces.

$$0 = C_{oo}^{(2)} + \sum_{n=1}^{\infty} \sum_{m=0}^{(n/4)} \left[C_{nm}^{(2)} F_{nm}^{(4)}(\mu) \cos(4m\phi) + C_{nm}^{(3)} G_{nm}^{(4)}(\mu) \cos(4m\phi) \right] \qquad \text{(III-25)}$$

where

$$F_{nm}^{(4)}(\mu) = \left(\frac{-1}{\mu} \right)^{n} P_n^{4m}(\mu)$$

$$G_{nm}^{(4)}(\mu) = \left(\frac{-1}{\mu} \right)^{-n-1} P_n^{4m}(\mu)$$

Equation (III-25) is valid under the following conditions

$$r = \frac{-1}{\mu}$$

$$-1 \leq \mu \leq \frac{-1}{(2 + \tan^2\phi)^{1/2}}$$

$$0 \leq \phi \leq \pi/4$$

The form of the three parts of the boundary condition applied to the top, side, and bottom faces is such that one

general equation may be written for the boundary condition. This equation is

$$H^{(4)}(\mu,\phi) = C_{oo}^{(2)} H^{(1)}(\mu,\phi) + \sum_{n=1}^{\infty} \sum_{m=0}^{(n/4)} \left[C_{nm}^{(2)} H_{nm}^{(2)}(\mu,\phi) + C_{nm}^{(3)} H_{nm}^{(3)}(\mu,\phi) \right] \tag{III-26}$$

The boundary condition on the outer face of the unit cell may be summarized in the following form.

Top Face:

$$r = \frac{1}{\mu}$$

$$\frac{1}{(2+\tan^2\phi)^{1/2}} \leq \mu \leq 1$$

$$0 \leq \phi \leq \frac{\pi}{4}$$

$$H^{(1)}(\mu,\phi) = 1$$

$$H_{nm}^{(2)}(\mu,\phi) = F_{nm}^{(1)}(\mu)\cos(4m\phi)$$

$$H_{nm}^{(3)}(\mu,\phi) = G_{nm}^{(1)}(\mu)\cos(4m\phi)$$

$$H^{(4)}(\mu,\phi) = 1$$

Side Face:

$$r = \frac{1}{\cos\phi\,(1-\mu^2)^{1/2}}$$

$$\frac{-1}{(2+\tan^2\phi)^{1/2}} \leq \mu \leq \frac{1}{(2+\tan^2\phi)^{1/2}}$$

$$0 \leq \phi \leq \frac{\pi}{4}$$

$$H^{(1)}(\mu,\phi) = 0$$

$$H_{nm}^{(2)}(\mu,\phi) = F_{nm}^{(2)}(\mu)\cos(4m\phi)\cos\phi + F_{nm}^{(3)}(\mu)\sin(4m\phi)\sin\phi$$

$$H_{nm}^{(3)}(\mu,\phi) = G_{nm}^{(2)}(\mu)\cos(4m\phi)\cos\phi + G_{nm}^{(3)}(\mu)\sin(4m\phi)\sin\phi$$

$$H^{(4)}(\mu,\phi) = 0$$

Bottom Face:

$$r = \frac{-1}{\mu}$$

$$1 \leq \mu \leq \frac{-1}{(2 + \tan^2\phi)^{1/2}}$$

$$0 \leq \phi \leq \frac{\pi}{4}$$

$$H^{(1)}(\mu, \phi) = 1$$

$$H^{(2)}_{nm}(\mu, \phi) = F^{(4)}_{nm}(\mu)\cos(4m\phi)$$

$$H^{(3)}_{nm}(\mu, \phi) = G^{(4)}_{nm}(\mu)\cos(4m\phi)$$

$$H^{(4)}(\mu, \phi) = 0$$

It now becomes necessary to work with equations (III-11), (III-14), (III-15), (III-17), (III-22), and (III-25) to determine the constants $C^{(1)}_{oo}$, $C^{(2)}_{oo}$, $C^{(1)}_{nm}$, $C^{(2)}_{nm}$ and $C^{(3)}_{nm}$.

C) Reduction to a System of Linear Algebraic Equations

Equation (III-26) is the general equation derived from applying the boundary condition to the outer faces of the unit cell. The next step is to solve for the coefficients in the temperature solutions by reducing equation (III-26) to a system of linear algebraic equations. This will be done by first defining $C_{nm}^{(2)}$ and $C_{nm}^{(3)}$ in terms of $C_{nm}^{(1)}$ ($C_{oo}^{(2)}$ is already defined in terms of $C_{oo}^{(1)}$), and then expanding the $H(\mu,\phi)$ functions in spherical harmonics.

Expansion of the four $H(\mu,\phi)$ functions in spherical harmonics as given by Prévost (6) gives the following equations:

$$H^{(1)}(\mu,\phi) = A1_{oo} + \sum_{\alpha=1}^{\infty}\sum_{\beta=0}^{(\alpha/4)} A1_{\alpha\beta}\, P_{\alpha}^{4\beta}(\mu)\cos(4\beta\phi)$$

$$H_{nm}^{(2)}(\mu,\phi) = A2_{oo}^{nm} + \sum_{\alpha=1}^{\infty}\sum_{\beta=0}^{(\alpha/4)} A2_{\alpha\beta}^{nm}\, P_{\alpha}^{4\beta}(\mu)\cos(4\beta\phi)$$

$$H_{nm}^{(3)}(\mu,\phi) = A3_{oo}^{nm} + \sum_{\alpha=1}^{\infty}\sum_{\beta=0}^{(\alpha/4)} A3_{\alpha\beta}^{nm}\, P_{\alpha}^{4\beta}(\mu)\cos(4\beta\phi)$$

$$H^{(4)}(\mu,\phi) = A4_{oo} + \sum_{\alpha=1}^{\infty}\sum_{\beta=0}^{(\alpha/4)} A4_{\alpha\beta}\, P_{\alpha}^{4\beta}(\mu)\cos(4\beta\phi)$$

(See Appendix D for derivations and solutions to expansion coefficients.)

From the boundary conditions that were applied at the sphere-cell interface, $r = R_a$, the following two equations

were derived.

$$C_{nm}^{(1)} R_a^n = C_{nm}^{(2)} R_a^n + C_{nm}^{(3)} R_a^{-n-1} \qquad \text{(III-27A)}$$

$$K_1 n C_{nm}^{(1)} R_a^{n-1} = K_2 \left(n C_{nm}^{(2)} R_a^{n-1} - (n+1) C_{nm}^{(3)} R_a^{-n-2} \right) \qquad \text{(III-27B)}$$

To state $C_{nm}^{(2)}$ and $C_{nm}^{(3)}$ in terms of $C_{nm}^{(1)}$, the first step is to solve both equations (III-27A) and (III-27B) for both $C_{nm}^{(2)}$ and $C_{nm}^{(3)}$.

$$C_{nm}^{(2)} = C_{nm}^{(1)} - C_{nm}^{(3)} R_a^{-2n-1} \qquad \text{(III-28A)}$$

$$C_{nm}^{(2)} = \frac{K_1}{K_2} C_{nm}^{(1)} + \left(\frac{n+1}{n} \right) R_a^{-2n-1} C_{nm}^{(3)} \qquad \text{(III-28B)}$$

$$C_{nm}^{(3)} = C_{nm}^{(1)} R_a^{2n+1} - C_{nm}^{(2)} R_a^{2n+1} \qquad \text{(III-28C)}$$

$$C_{nm}^{(3)} = -\frac{K_1}{K_2} \left(\frac{n}{n+1} \right) R_a^{2n+1} C_{nm}^{(1)} + \left(\frac{n}{n+1} \right) R_a^{2n+1} C_{nm}^{(2)} \qquad \text{(III-28D)}$$

Now setting equation (III-28A) equal to equation (III-28B) and solving for $C_{nm}^{(3)}$

$$C_{nm}^{(3)} = \frac{C_{nm}^{(1)} \left(1 - \frac{K_1}{K_2} \right) n R_a^{2n+1}}{2n+1} \qquad \text{(III-29)}$$

And setting equation (III-28C) equal to equation (III-28D) and solving for $C_{nm}^{(2)}$

$$C_{nm}^{(2)} = C_{nm}^{(1)} \left(\frac{K_2 (n+1) + K_1 n}{K_2 (2n+1)} \right) \qquad \text{(III-30)}$$

The expressions for $C_{oo}^{(2)}$, $C_{nm}^{(2)}$, $C_{nm}^{(3)}$, $H^{(1)}(\mu,\phi)$, $H_{nm}^{(2)}(\mu,\phi)$, $H_{nm}^{(3)}(\mu,\phi)$ and $H^{(4)}(\mu,\phi)$ are now inserted into equation (III-26). This yields the following expression:

$$C_{oo}^{(1)}\left[A1_{oo}+\sum_{\alpha=1}^{\infty}\sum_{\beta=0}^{(\alpha/4)}A1_{\alpha\beta}\,P_{\alpha}^{4\beta}(\mu)\cos(4\beta\phi)\right]+\sum_{n=1}^{\infty}\sum_{m=0}^{(n/4)}\left\{C_{nm}^{(1)}\left(\frac{K_2(n+1)+K_1 n}{K_2(2n+1)}\right)\right.$$

$$\cdot\left[A2_{oo}^{nm}+\sum_{\alpha=1}^{\infty}\sum_{\beta=0}^{(\alpha/4)}A2_{\alpha\beta}^{nm}\,P_{\alpha}^{4\beta}(\mu)\cos(4\beta\phi)\right]+C_{nm}^{(1)}\,\frac{\left(1-\frac{K_1}{K_2}\right)n\,R_a^{2n+1}}{2n+1}$$

$$\left.\cdot\left[A3_{oo}^{nm}+\sum_{\alpha=1}^{\infty}\sum_{\beta=0}^{(\alpha/4)}A3_{\alpha\beta}^{nm}\,P_{\alpha}^{4\beta}(\mu)\cos(4\beta\phi)\right]\right\}=A4_{oo}+\sum_{\alpha=1}^{\infty}\sum_{\beta=0}^{(\alpha/4)}A4_{\alpha\beta}\,P_{\alpha}^{4\beta}(\mu)\cos(4\beta\phi)$$

(III-31)

By using the orthogonal properties of the cosine function and the associated Legendre function, it is possible to reduce equation (III-31) to a system of linear equations dependent upon n and m. First operating upon equation (III-31) with $\int_0^{\pi/4}\cos(4\eta\phi)\,d\phi$ where

$$\int_0^{\pi/4}\cos(4\eta\phi)\,d\phi=\begin{cases}\pi/4 & ,\ \eta=0\\ 0 & ,\ \eta\neq 0\end{cases}$$

and where

$$\int_0^{\pi/4}\cos(4\beta\phi)\cos(4\eta\phi)\,d\phi=\begin{cases}\pi/8 & ,\ \eta=\beta\\ 0 & ,\ \eta\neq\beta\end{cases}$$

This gives the following result.

$$C_{oo}^{(1)}\sum_{\alpha=1}^{\infty}A1_{\alpha\eta}\,P_{\alpha}^{4\eta}(\mu)+\sum_{n=1}^{\infty}\sum_{m=0}^{(n/4)}\left\{C_{nm}^{(1)}\left(\frac{K_2(n+1)+K_1 n}{K_2(2n+1)}\right)\sum_{\alpha=1}^{\infty}A2_{\alpha\eta}^{nm}\,P_{\alpha}^{4\eta}(\mu)\right.$$

$$\left.+C_{nm}^{(1)}\,\frac{\left(1-\frac{K_1}{K_2}\right)n\,R_a^{2n+1}}{2n+1}\sum_{\alpha=1}^{\infty}A3_{\alpha\eta}^{nm}\,P_{\alpha}^{4\eta}(\mu)\right\}=\sum_{\alpha=1}^{\infty}A4_{\alpha\eta}\,P_{\alpha}^{4\eta}(\mu)$$

Now operating with $\int_{-1}^{1}P_r^{4\eta}(\mu)\,d\mu$

where

$$\int_{-1}^{1} P_\alpha^{4\eta}(\mu)\, P_\gamma^{4\eta}(\mu)\, d\mu = \begin{cases} \dfrac{2}{2\gamma+1}\,\dfrac{(\gamma+4\eta)!}{(\gamma-4\eta)!} & , \gamma = \alpha \\ 0 & , \gamma \neq \alpha \end{cases}$$

This produces

$$A1_{\gamma\eta}\, C_{oo}^{(1)} + \sum_{n=1}^{\infty}\sum_{m=0}^{(n/4)} \left\{ A2_{\gamma\eta}^{nm} \left(\frac{K_2(n+1)+K_1 n}{K_2(2n+1)} \right) C_{nm}^{(1)} \right.$$

$$\left. + A3_{\gamma\eta}^{nm} \left(\frac{\left(1-\frac{K_1}{K_2}\right) n\, R_a^{2n+1}}{2n+1} \right) C_{nm}^{(1)} \right\} = A4_{\gamma\eta}$$

which may be finally simplified to

$$A1_{\gamma\eta} C_{oo}^{(1)} + \sum_{n=1}^{\infty}\sum_{m=0}^{(n/4)} \left\{ C_{nm}^{(1)} \left[A2_{\gamma\eta}^{nm} \left(\frac{K_2(n+1)+K_1 n}{K_2(2n+1)} \right) \right.\right.$$

$$\left.\left. + \frac{A3_{\gamma\eta}^{nm}\left(1-\frac{K_1}{K_2}\right) n\, R_a^{2n+1}}{2n+1} \right] \right\} = A4_{\gamma\eta} \qquad \text{(III-32)}$$

The problem of finding the constants in the temperature solutions for the unit cell has now been reduced to a system of linear algebraic equations as defined by equation (III-32). For numerical evaluation an upper limit on n will be chosen. This represents how many terms will be kept in the expansion for the solution to the temperature constants.

Equation (III-32) will be used to determine the constants $C_{oo}^{(1)}$, $C_{10}^{(1)}$, ... to $C_{nm}^{(1)}$. Once these constants have been determined, it is possible to obtain $C_{oo}^{(2)}$, $C_{nm}^{(2)}$ and $C_{nm}^{(3)}$ from equations (III-14), (III-29), and (III-30).

Once all constants in the solutions for the temperature (equations (III-6) and (III-7)) have been determined, the temperature at any point within the unit cell may be evaluated.

IV. RESULTS

To be able to use the analytical method of determining temperatures that was presented in the preceding section, it is necessary to develop a code for use upon a digital computer. Such a code, TEMPRO, was developed, and calculates temperatures for the unit cell used in this analysis. The code involves all necessary operations to produce equation (III-32) and then solves that equation for the constants $C_{oo}^{(1)}$ and $C_{nm}^{(1)}$. Once the code has determined those constants it can calculate all other necessary constants and can solve for the temperatures in the unit cell as defined by equations (III-6) and (III-7). As an aid to check the operation of TEMPRO, the heat flux on the side face of the unit cell, as defined by equation (III-21), is also calculated. Appendix E provides a further description and a listing of TEMPRO.

The method used to analyze the operation of TEMPRO will be to check on the return of the input boundary conditions. This method will be used since on the faces it is possible to check directly how well the solutions return the given boundary conditions.

There are three conditions which will therefore be

checked. Those conditions are the continuity of temperature at the sphere-cube interface, the temperature on the top and bottom planes, and the heat flux on the side face. The continuity of temperature at the sphere-cube interface was always found to be returned exactly for any unit cell conditions which were investigated. This result was expected because this boundary condition is easiest to satisfy as there is no intermixing of the spherical and cubical geometrics involved in its satisfaction. A boundary condition of constant temperatures on the top and bottom faces was applied during this investigation for two reasons. First, an experimental arrangement to check the theoretical modeling may be most easily designed with constant temperatures, and, secondly, it is simpler to check the return of a boundary condition if it is a constant rather than a varying function. The results from TEMPRO show that the returned temperature profiles on the top and bottom faces are symmetrical, so analysis of the temperature boundary conditions will be limited to the top face of the unit cell. The third boundary condition of interest is the adiabatic side face. In general it was found that the average heat flux on the side face was equal to zero, plus or minus 10^{-5} W/cm^2.

The point values of the side face heat flux were found to be symmetrical around the center plane (Z = 0) of the unit cell.

To provide a means of determining how well the boundary conditions are returned, three basic parameters will be used. The first parameter will be the average temperature on the top face. This average temperature ($\bar{T}_T$) will be calculated by:

$$\bar{T}_T = \frac{\sum_{i=1}^{N} T_{Ti}}{N}$$

where T_{Ti} is the returned temperature at each grid point on the top face and N is the number of grid points. This average returned temperature will be compared to the input temperature boundary condition (θ_T) and will be a measure of how closely the input condition was returned. The second and third parameters to be used are the standard deviations of the returned top face temperature and the returned side face heat flux. These will be calculated through the use of the general equation:

$$\sigma = \left(\frac{\sum_{i=1}^{N} \left(A_i - \bar{A} \right)^2}{N} \right)^{1/2}$$

where σ is the standard deviation, A_i is the individual value, $\bar{A}$ is the mean value, and N is the number of points. Respectively for the top face temperature and the side face

heat flux, the symbols used will be σ_T and σ_ϕ, T_{Ti} and ϕ_i, and $\overline{T}_T$ and $\overline{\phi}$, for σ, A_i and $\overline{A}$. The use of the standard deviation provides a measure of how much deviation occurs between specific values of the temperature or the heat flux. This will be useful as it is possible for two separate unit cells to return the same average values, but one will have point values with a greater dispersion about the mean value. It may then be concluded that the results are better in the case with the lower dispersion.

Computer data was obtained from varying the four basic inputs to the code. Those inputs are 1) the number of terms to be used in the summation, 2) the size of the sphere in relation to the size of the cube, 3) the thermal conductivities of both materials in the unit cell, and 4) the temperatures on both the top and bottom planes of the unit cell. The parameters $\overline{T}_T$, σ_T and σ_ϕ are then used to determine the conditions and effects due to changing inputs.

A) Effect of the Number of Terms Carried in the Summation

It was expected, prior to operation of the computer code, that the returned values of the boundary conditions would asymptotically approach the input conditions as the

number of terms (n) was increased, i.e., $\bar{T}_T \rightarrow \theta_T$, $\sigma_T \rightarrow 0$ and $\sigma_\phi \rightarrow 0$. As may be seen in Table 1 and Figure 7, this did not occur in actual operation of TEMPRO. Table 1 lists no results for even values of n because it was found that even values of n would return the same answers, to six significant digits, as the next lowest odd value of n (i.e., n = 4 and n = 3). By observation it was seen that additional terms due to the even value of n were several orders of magnitude smaller than the terms already present from the next lowest odd value of n, and therefore made little contribution to the answers.

It was decided to run TEMPRO with five terms for all further investigation as based on the data obtained from varying n. Observation shows that with n equal five there is the lowest deviation from the input conditions. The last column in Table 1 provides a numerical evaluation of the deviation from input conditions for each case. Operation of TEMPRO was limited to a maximum of nine terms for one primary reason, computer time versus number of terms increased exponentially and operation would become prohibitively expensive for greater than nine terms.

Some specific base conditions were selected to be maintained while varying other inputs during further computer

TABLE 1

RETURNED ACCURACY VERSUS NUMBER OF TERMS IN SUMMATION

n	$\overline{T_T}$ (°C)	σ_T (°C)	σ_ϕ (W/cm²)	$\lvert\overline{T_T} - \theta_T\rvert + \sigma_T + \sigma_\phi$
1	508.0903	1.5121	0.2829	3.7407
3	510.9231	2.2101	0.3653	3.4985
5	510.6788	1.9519	0.4522	3.0829
7	508.2520	2.4784	0.3962	4.6226
9	509.8095	3.2762	0.7177	4.1844

$K_1 = 0.16$ W/cm°C, $K_2 = 0.002$ W/cm°C, $R_s/R_c = 1$,

$\theta_T = 510$°C, $\theta_B = 500$°C

$K_1 = 0.16$ W/cm°C, $K_2 = 0.002$ W/cm°C, $R_s/R_c = 1$
$\theta_T = 510°C$, $\theta_B = 500°C$

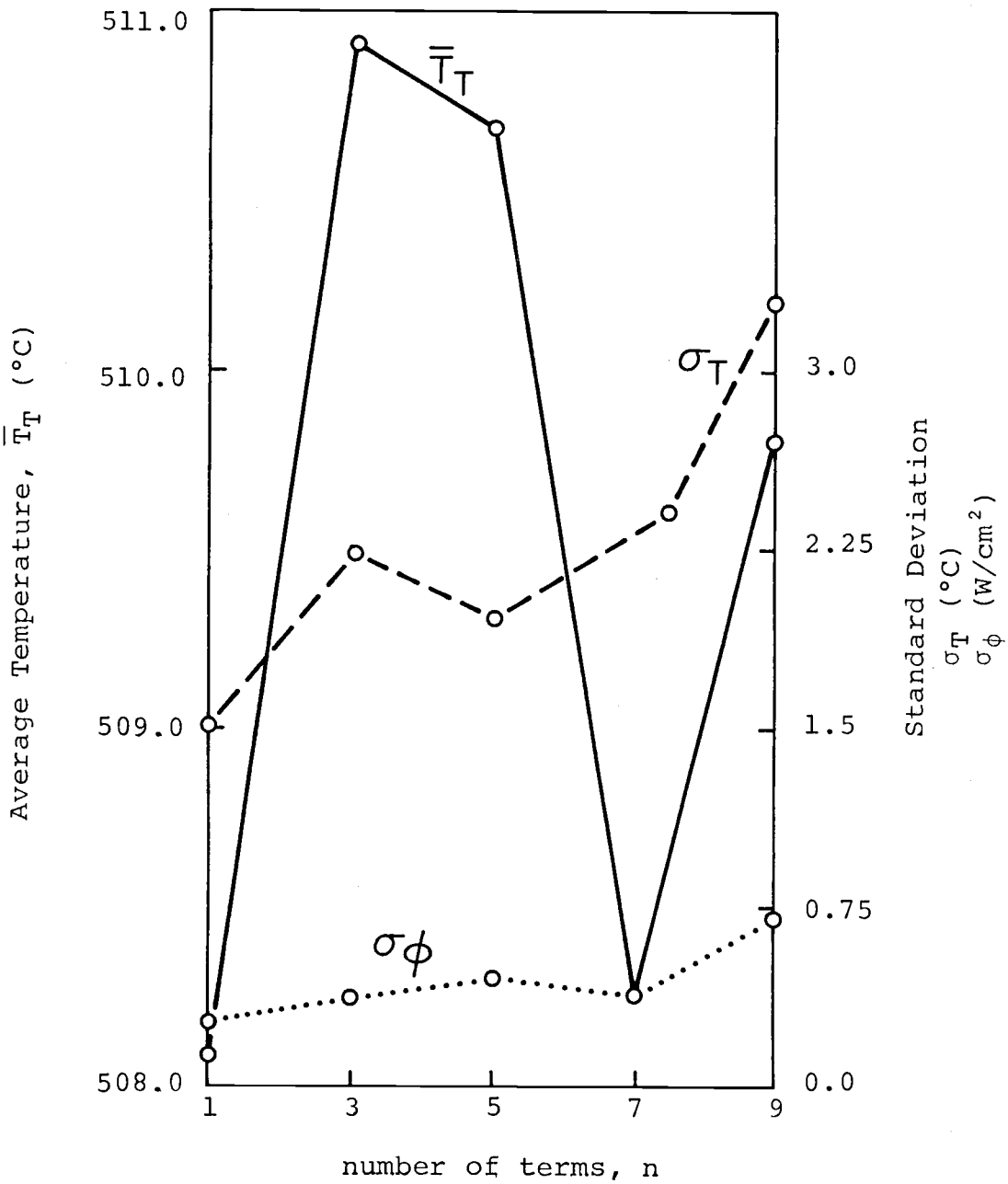

Figure 7: Returned accuracy versus number of terms in summation

operation. First, five terms were used in all runs. Second, thermal conductivities of 0.16 and 0.002 W/cm°C were chosen as base values. These are the thermal conductivities of uranium carbide and helium gas respectively at approximately 500°C. Lastly, a top temperature of 510°C and a bottom temperature of 500°C were chosen as base conditions. A temperature change of 10°C was chosen so as to reduce any temperature dependent thermal conductivity effects.

B) Effect of the Size of the Sphere in Relation to the Size of the Cube

Because of the non-dimensionalizing of distance in the analytical development of the temperature solutions, the true values that are input for the size of the sphere and the cube make no difference in the results. The factor that is of importance here is the ratio of the sphere radius to the cube radius (R_S/R_C). It was quickly found that a ratio equal to one produces the maximum deviation from input conditions when considering the effect of the radius ratio. If the radius of the sphere is zero, then the unit cell becomes a homogeneous cube. Under these conditions exact

values of the boundary conditions were returned and all interior temperatures agree perfectly with one-dimensional slab theory, that is, a linear variation in temperature between the top and bottom planes and constant temperature on all planes parallel to the top and bottom faces.

One factor that must be considered concurrently with the radius ratio is whether the sphere or the remaining cell has the larger conductivity. Table 2 and Figure 8 show results for varying the radius ratio when the sphere conductivity is greater than the cell conductivity. By interpolation from Figure 8 it is seen that σ_T and σ_ϕ have dropped to one half, or less, their value when $R_s/R_c = 1$, when the radius ratio has decreased to 0.94. When the sphere conductivity is less than the cell conductivity, it is seen that the deviations are less at all values of the radius ratio than for the opposite case, but that the amount of deviation reduces at a lower rate. Table 3 and Figure 9 show the results of varying the radius ratio when $K_1 < K_2$. By interpolation from Figure 9 it was found that at $R_s/R_c = 0.85$ σ_T and σ_ϕ are one half, or less, their values at $R_s/R_c = 1$. It is conjectured that better results are obtained when the cell conductivity is larger because a more homogeneous situation is present when the material

TABLE 2

RETURNED ACCURACY VERSUS RADIUS RATIO, $K_1 > K_2$

R_s/R_c	$\bar{T}_T$ (°C)	σ_T (°C)	σ_ϕ (W/cm^2)
1.0	510.6788	1.9519	0.4522
0.9	510.5610	0.7748	0.1702
0.8	510.4004	0.5142	0.0945
0.7	510.2575	0.3282	0.0558
0.6	510.1538	0.1960	0.0323
0.5	510.0851	0.1082	0.0177
0.4	510.0421	0.0541	0.0087
0.3	510.0174	0.0224	0.0036
0.2	510.0051	0.0000	0.0010
0.1	510.0006	0.0000	0.0001
0.0	510.0000	0.0000	0.0000

K_1 = 0.16 W/cm°C, K_2 = 0.002 W/cm°C, θ_T = 510°C,

θ_B = 500°C, n = 5

K_1 = 0.16 W/cm°C, K_2 = 0.002 W/cm°C,
θ_T = 510°C, θ_B = 500°C, n = 5

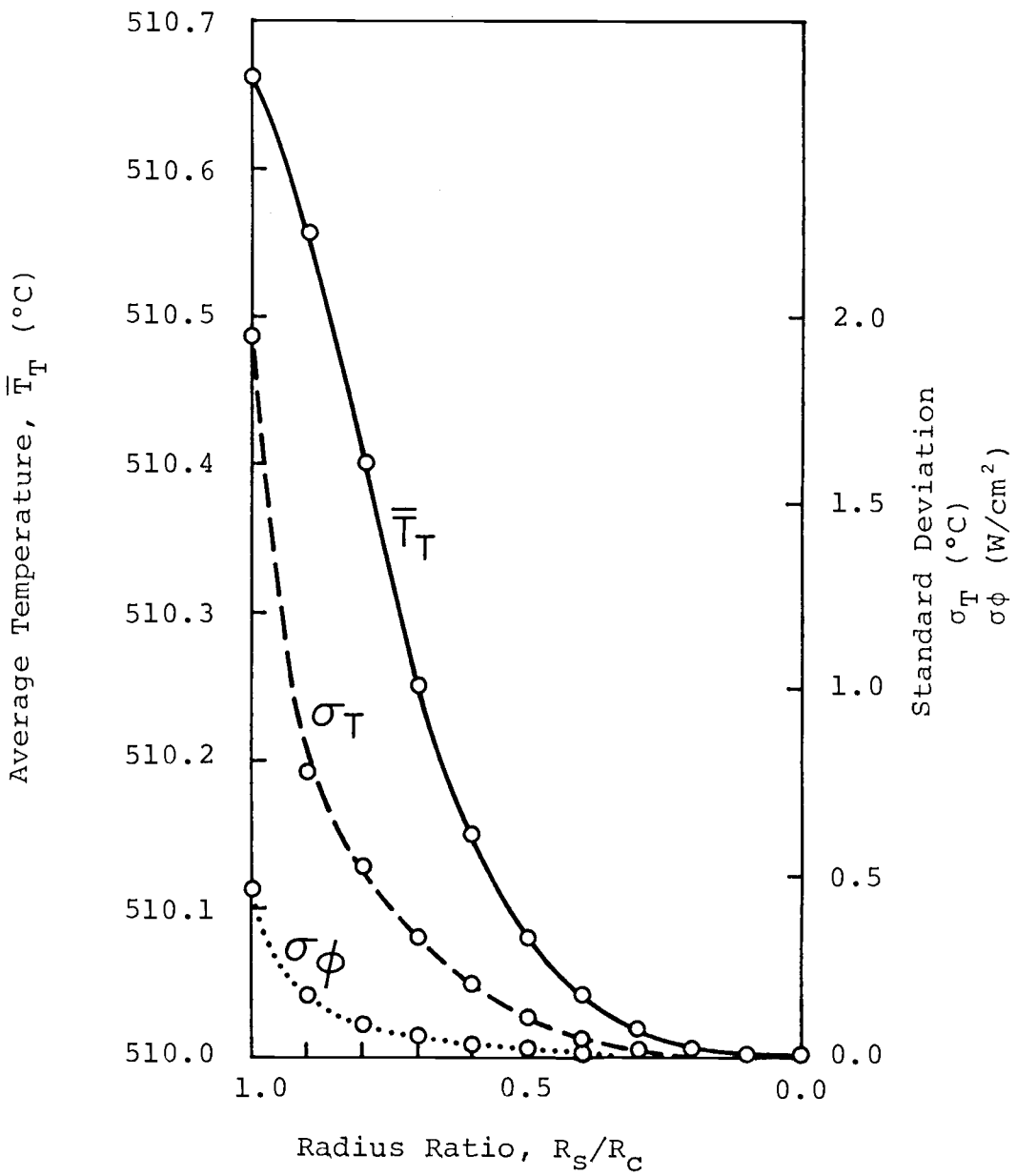

Figure 8: Returned accuracy versus radius ratio, $K_1 > K_2$

TABLE 3

RETURNED ACCURACY VERSUS RADIUS RATIO, $K_1 < K_2$

R_s/R_c	$\bar{T}_T$ (°C)	σ_T (°C)	σ_ϕ (W/cm^2)
1.0	509.5579	0.5943	0.0759
0.9	509.7504	0.3234	0.0448
0.8	509.8401	0.2042	0.0308
0.7	509.8951	0.1334	0.0211
0.6	509.9334	0.0858	0.0136
0.5	509.9608	0.0493	0.0081
0.4	509.9796	0.0267	0.0042
0.3	509.9913	0.0085	0.0018
0.2	509.9974	0.0000	0.0005
0.1	509.9996	0.0000	0.0001
0.0	510.0000	0.0000	0.0000

K_1 = 0.002 W/cm°C, K_2 = 0.16 W/cm°C, θ_T = 510°C, θ_B = 500°C, n = 5

K_1 = 0.002 W/cm°C, K_2 = 0.16 W/cm°C,
θ_T = 510°C, θ_B = 500°C, n = 5

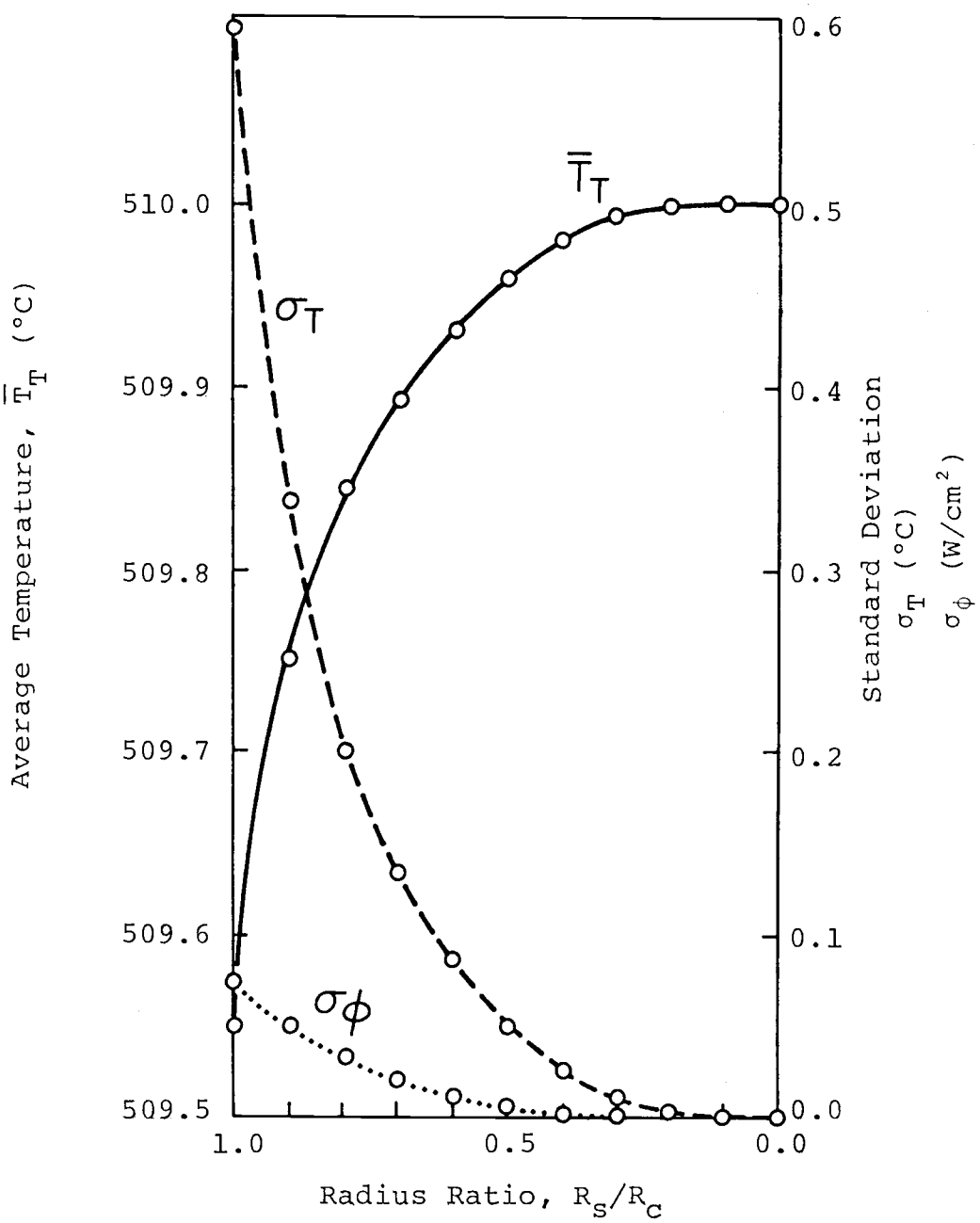

Figure 9: Returned accuracy versus radius ratio, $K_1 < K_2$

outside of the sphere has the larger conductivity.

C) Effect of the Thermal Conductivities of the Two Materials

Investigation of the effect on the return of the boundary conditions due to changing the thermal conductivities of the two regions was performed by varying the conductivity of one region while holding the other region constant. Each region was held at 0.16 W/cm°C while the other region was varied from 0.001-0.16 W/cm°C. As was initially expected, it was found that the ratio of the conductivities, when considering the effect of the conductivities, was the controlling factor in the accuracy of the return of the boundary conditions. As the ratio approaches a value of one, the average temperature on the top face approaches the input boundary condition and both standard deviations approach zero. At a conductivity ratio of one, all boundary conditions are returned exactly (for any radius ratio) and the results agree with one-dimensional slab theory. This result is supportive of the conclusion that the analytical solution for the temperatures is valid and that the deviation in answers for the non-homogeneous unit cell is likely due to trying to merge a sphere and a cube into a single

TABLE 4

RETURNED ACCURACY VERSUS CELL CONDUCTIVITY, $K_1 \geq K_2$

K_2 (W/cm°C)	K_1/K_2	$\bar{T}_T$ (°C)	σ_T (°C)	σ_ϕ (W/cm²)
0.0010	160.00	510.7083	2.1079	0.4859
0.0025	64.00	510.6652	1.8814	0.4369
0.0050	32.00	510.6066	1.5864	0.3724
0.0075	21.33	510.5597	1.3634	0.3228
0.0100	16.00	510.5237	1.1880	0.2837
0.0250	6.40	510.3739	0.6474	0.1553
0.0500	3.20	510.2453	0.3453	0.0771
0.0750	2.13	510.1636	0.2146	0.0435
0.1000	1.60	510.1027	0.1323	0.0245
0.1600	1.00	510.0000	0.0000	0.0000

K_1 = 0.16 W/cm°C, R_S/R_C = 1, θ_T = 510°C, θ_B = 500°C,

n = 5

TABLE 5

RETURNED ACCURACY VERSUS ΔK AND K_1/K_2, $K_1 \geq K_2$

K_1 (W/cm°C)	K_2 (W/cm°C)	ΔK (W/cm°C)	K_1/K_2	$\overline{T_T}$ (°C)	σ_T (°C)	σ_ϕ (W/cm²)
0.2	0.05	0.15	4.00	510.2882	0.4300	0.0994
0.3	0.15	0.15	2.00	510.1501	0.1958	0.0389
0.4	0.25	0.15	1.60	510.1027	0.1323	0.0245
4.0	0.20	3.80	20.0	510.5514	1.3252	0.3143
0.2	0.01	0.19	20.0	510.5514	1.3252	0.3143
20.0	1.00	19.00	20.0	510.5514	1.3252	0.3143

$R_S/R_C = 1$, $\theta_T = 510°C$, $\theta_B = 500°C$, $n = 5$

K_1 = 0.16 W/cm°C, R_s/R_c = 1.0,
θ_T = 510°C, θ_B = 500°C, n = 5

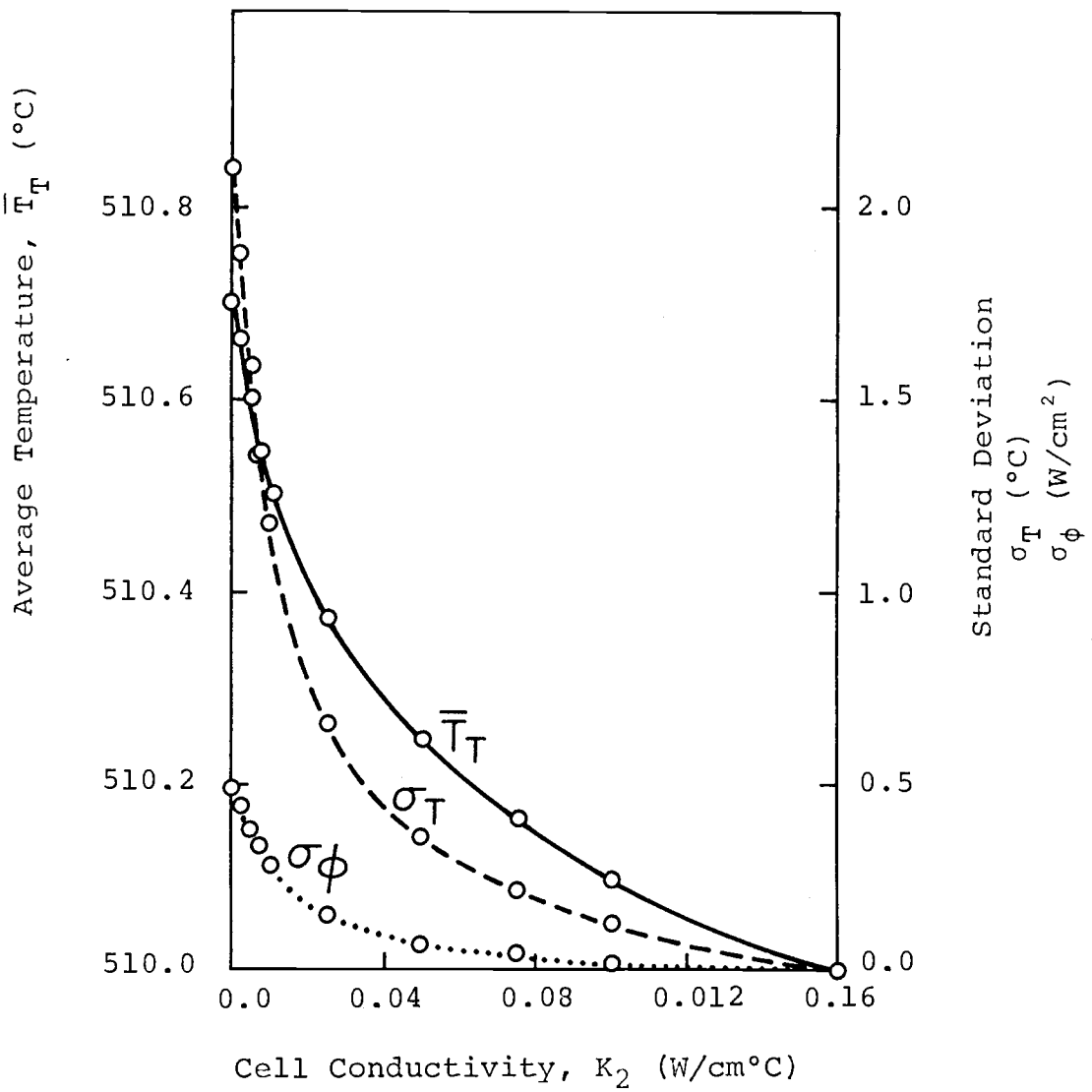

Figure 10: Returned accuracy versus cell conductivity, $K_1 \geq K_2$

K_1 = 0.16 W/cm°C, R_s/R_c = 1.0,
θ_T = 510°C, θ_B = 500°C, n = 5

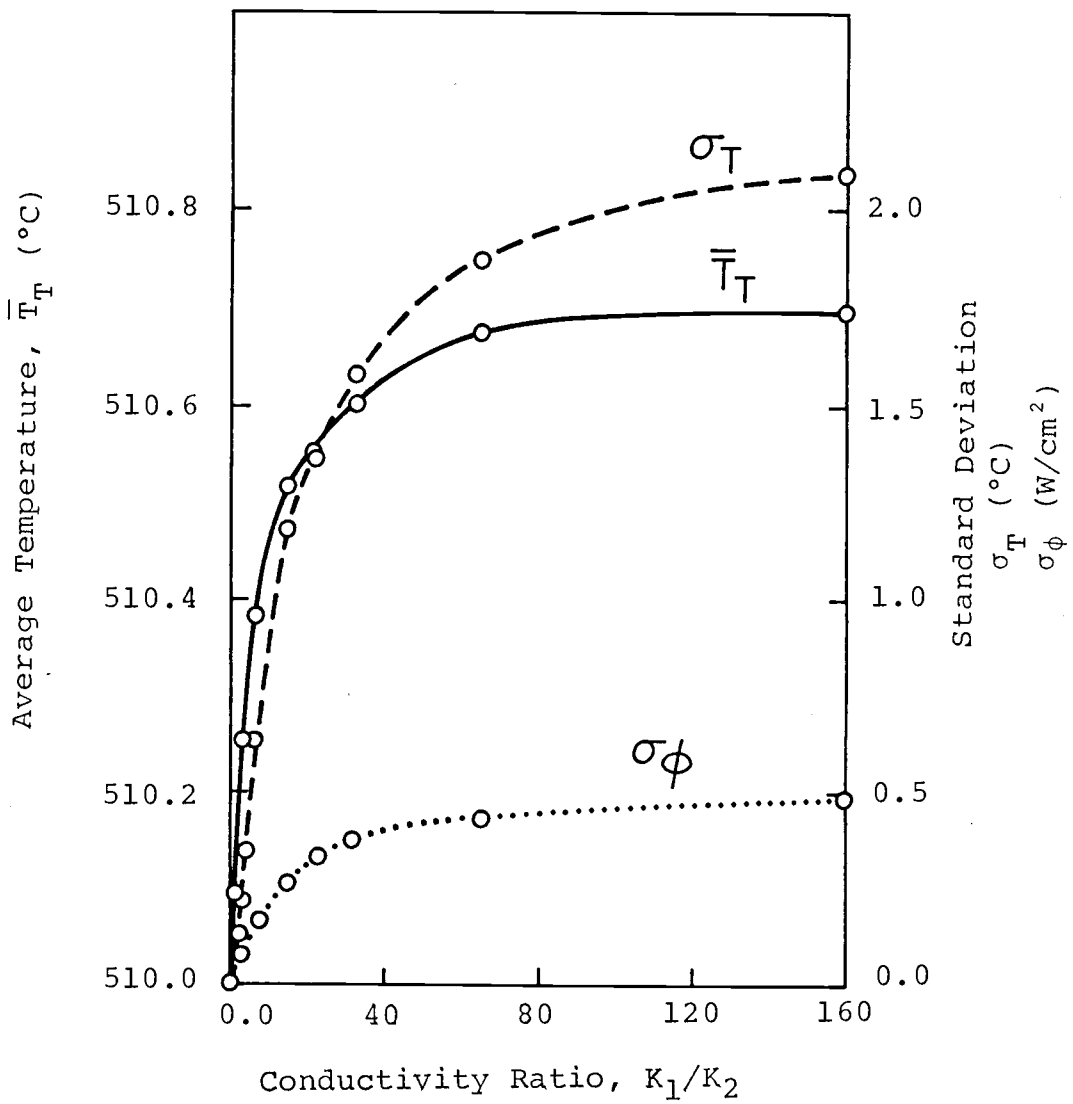

Figure 11: Returned accuracy versus conductivity ratio, $K_1 \geq K_2$

TABLE 6

RETURNED ACCURACY VERSUS SPHERE CONDUCTIVITY, $K_1 \leq K_2$

k_1 (W/cm°C)	k_2/k_1	$\bar{T}_T$ (°C)	σ_T (°C)	σ_Φ (W/cm²)
0.0010	160.00	509.5520	0.6028	0.0769
0.0025	64.00	509.5608	0.5902	0.0754
0.0050	32.00	509.5751	0.5702	0.0730
0.0075	21.33	509.5890	0.5507	0.0706
0.0100	16.00	509.6023	0.5320	0.0684
0.0250	6.40	509.6739	0.4326	0.0565
0.0500	3.20	509.7682	0.3037	0.0411
0.0750	2.13	509.8408	0.2062	0.0291
0.1000	1.60	509.8987	0.1301	0.0192
0.1600	1.00	510.0000	0.0000	0.0000

K_2 = 0.16 W/cm°C, R_S/R_C = 1, θ_T = 510°C, θ_B = 500°C, n = 5

TABLE 7

RETURNED ACCURACY VERSUS ΔK AND K_2/K_1, $K_1 \leq K_2$

K_1 (w/cm°c)	K_2 (w/cm°c)	ΔK (w/cm°c)	K_2/K_1	$\bar{T}_T$ (°c)	σ_T (°c)	σ_ϕ (w/cm²)
0.05	0.2	0.15	4.0	509.7336	0.3505	0.0468
0.25	0.4	0.15	1.6	509.8987	0.1301	0.0192
0.01	2.0	9.90	20	509.5508	0.6043	0.0771
1.00	20.0	19.00	20	509.5917	0.5470	0.0702

$R_S/R_C = 1$, $\theta_T = 510°C$, $\theta_B = 500°C$, $n = 5$

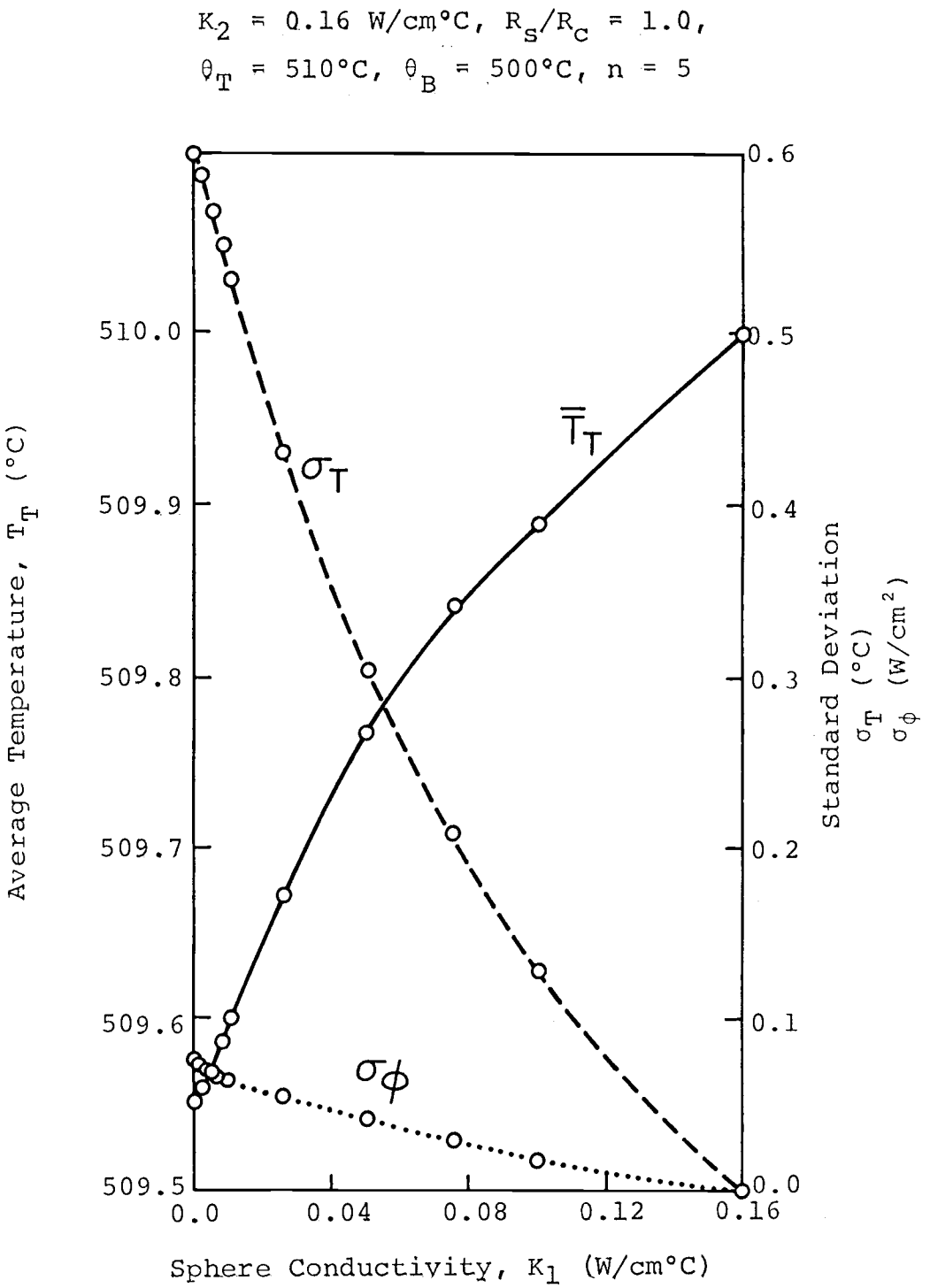

Figure 12: Returned accuracy versus sphere conductivity $K_1 \leq K_2$

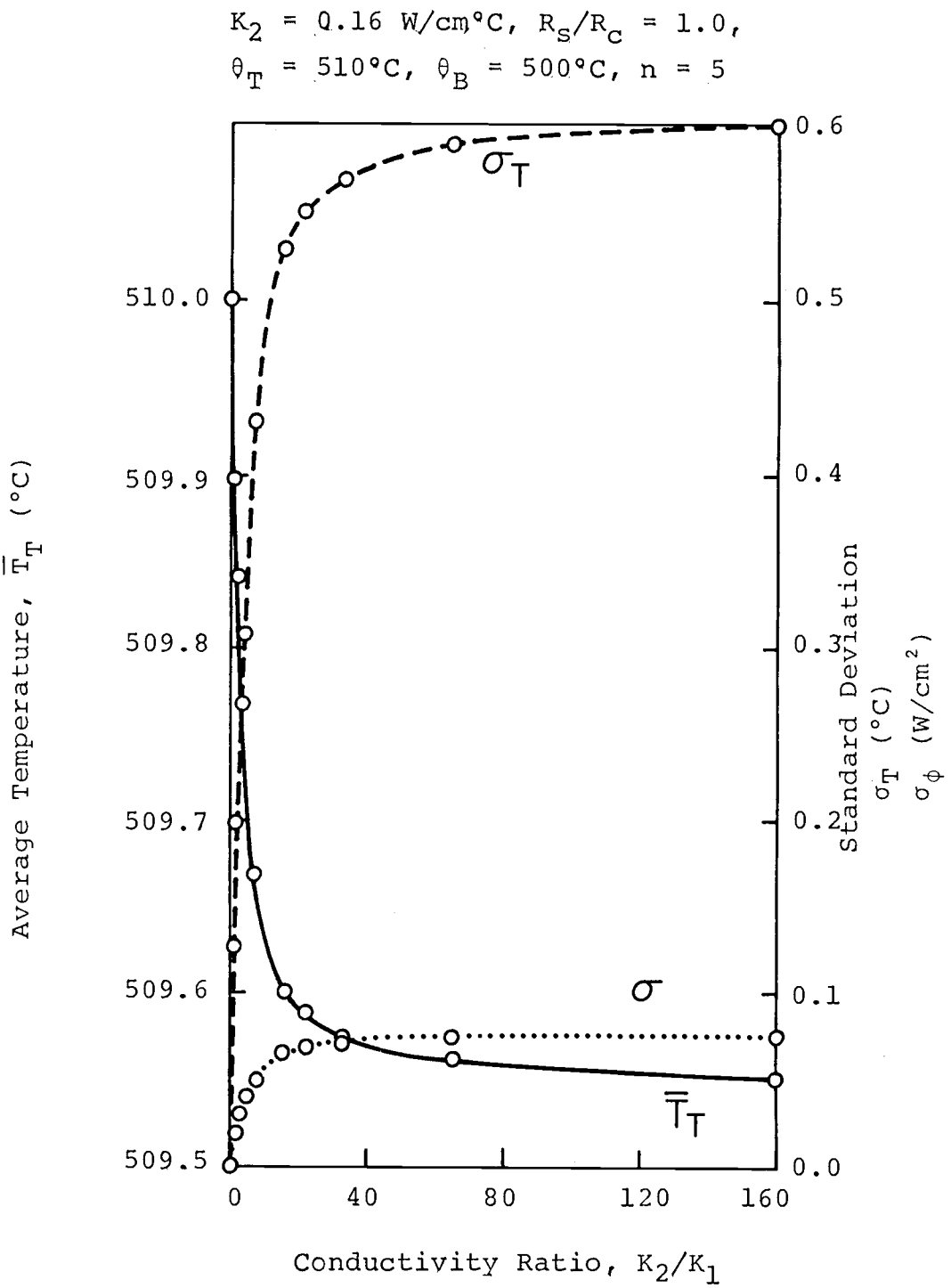

Figure 13: Returned accuracy versus conductivity ratio, $K_1 \leq K_2$

unit cell.

Computer data was obtained for the two cases $K_1 \geq K_2$ and $K_1 \leq K_2$. Tables 4-5 and Figures 10-11 compile the results when the sphere is at a constant conductivity while the remaining cell varies in conductivity (case 1). Tables 6-7 and Figures 12-13 pertain to case 2 where the sphere conductivity varies while the remaining cell is maintained at constant conductivity. For case 1, $K_1 \geq K_2$, it was found that for constant conductivity ratio, the computer results were constant and independent of the absolute values of the two conductivities. It was then expected that a similar result would hold for case 2 ($K_1 \leq K_2$). However, as shown by Table 7, this did not occur, but that accuracy was improved as the value of K_1 was increased. Comparison of Figures 11 and 13 shows that case 2 has lower deviation from the input conditions. This supports the conjecture that better results are obtained and a more homogeneous unit cell is produced when the volume surrounding the sphere has the higher thermal conductivity of the two regions.

D) Effect of the Temperature Boundary Conditions

The last input condition which can have an effect is the specified temperature on the top and bottom faces of

the unit cell. As the temperature was non-dimensionalized in the analytical development, it was expected that the absolute temperature would have no effect on the return of the input conditions by the computer code. It was quickly concluded that the difference in the input conditions, $\Delta\theta = \theta_T - \theta_B$, was the governing factor when considering the effect of the temperature boundary conditions. As proof of this it was seen for constant $\Delta\theta$ that the temperature and heat flux standard deviations were constant, as was the difference between the calculated average temperature on the top face and the input boundary condition.

Tables 8-9 and Figures 14-15 show the results of the computer data that was obtained. Through the use of a least squares fit to the data, it was found that the plots of $\overline{T}_T - \theta_T$ and σ_T versus $\Delta\theta$ for $K_1 > K_2$ have slopes of 6.7878 $\times 10^{-2}$ and 1.9519$\times 10^{-1}$ respectively. They both pass through the origin as would be expected.

For the case where $K_2 > K_1$, linear plots are also obtained for the plots of $\overline{T}_T - \theta_T$ and σ_T versus $\Delta\theta$. Those plots pass through the origin as expected and have slopes of 4.421$\times 10^{-2}$ and 5.943$\times 10^{-2}$ respectively. As has been found in the investigations of the other parameters, when the cell

TABLE 8

RETURNED ACCURACY VERSUS

TEMPERATURE BOUNDARY CONDITIONS, $K_1 > K_2$

θ_T (°C)	θ_B (°C)	$\Delta\theta$ (°C)	$\bar{T}_T$ (°C)	$\lvert\bar{T}_T - \theta_T\rvert$ (°C)	σ_T (°C)	σ_ϕ (W/cm²)
510	500	10	510.6788	0.6788	1.9519	0.4522
525	500	25	526.6970	1.6970	4.8799	0.4522
550	500	50	553.3939	3.3939	9.7597	0.4522
575	500	75	580.0909	5.0909	14.640	0.4522
600	500	100	606.7879	6.7879	19.519	0.4522
650	500	150	660.1818	10.1818	29.279	0.4522
700	500	200	713.5757	13.5757	39.039	0.4522
10	0	10	10.6788	0.6788	1.9519	0.4522
100	0	100	106.7879	6.7879	19.519	0.4522

K_1 = 0.16 W/cm°C, K_2 = 0.002 W/cm°C, R_S/R_C = 1, n = 5

TABLE 9

RETURNED ACCURACY VERSUS

TEMPERATURE BOUNDARY CONDITIONS, $K_1 < K_2$

Θ_T (°C)	Θ_B (°C)	$\Delta\Theta$ (°C)	$\bar{T}_T$ (°C)	$\lvert\bar{T}_T - \Theta_T\rvert$ (°C)	σ_T (°C)	σ_Φ (W/cm²)
505	500	5	504.7790	0.2210	0.2972	0.0759
510	500	10	509.5579	0.4421	0.5943	0.0759
525	500	25	523.8948	1.1052	1.4859	0.0759
550	500	50	547.7895	2.2105	2.9717	0.0759
575	500	75	571.6643	3.3357	4.4380	0.0759
600	500	100	595.5790	4.4210	5.9433	0.0759
650	500	150	643.3686	6.6314	8.9150	0.0759
700	500	200	691.1581	8.8419	11.886	0.0759

K_1 = 0.002 W/cm°C, K_2 = 0.16 W/cm°C, R_s/R_c = 1, n = 5

K_1 = 0.16 W/cm°C, K_2 = 0.002 W/cm°C, R_s/R_c = 1.0, n = 5

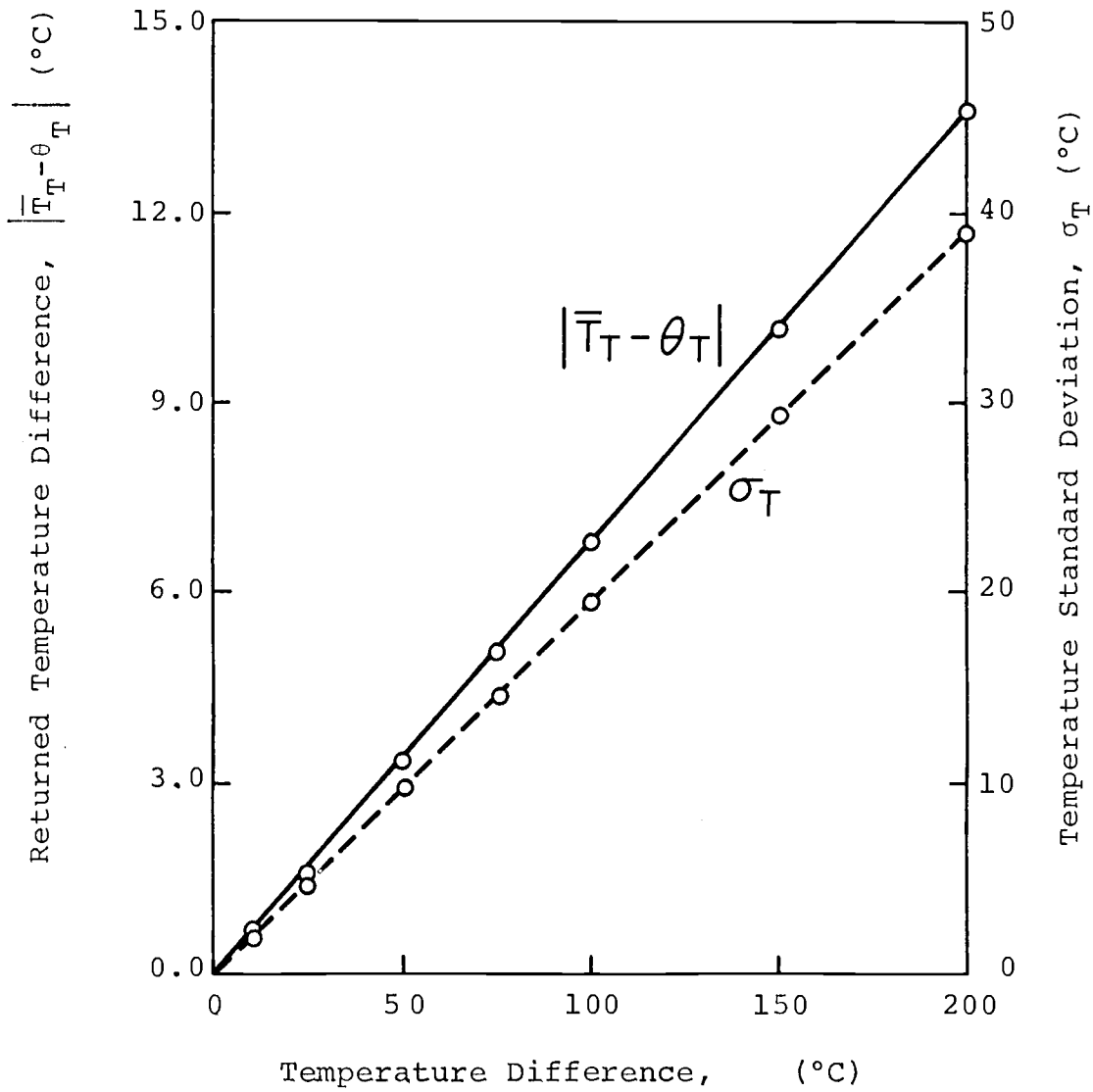

Figure 14: Returned accuracy versus temperature difference ($\Delta\theta$), $K_1 > K_2$

K_1 = 0.002 W/cm^2, K_2 = 0.16 W/cm°C, R_s/R_c = 1.0, n = 5

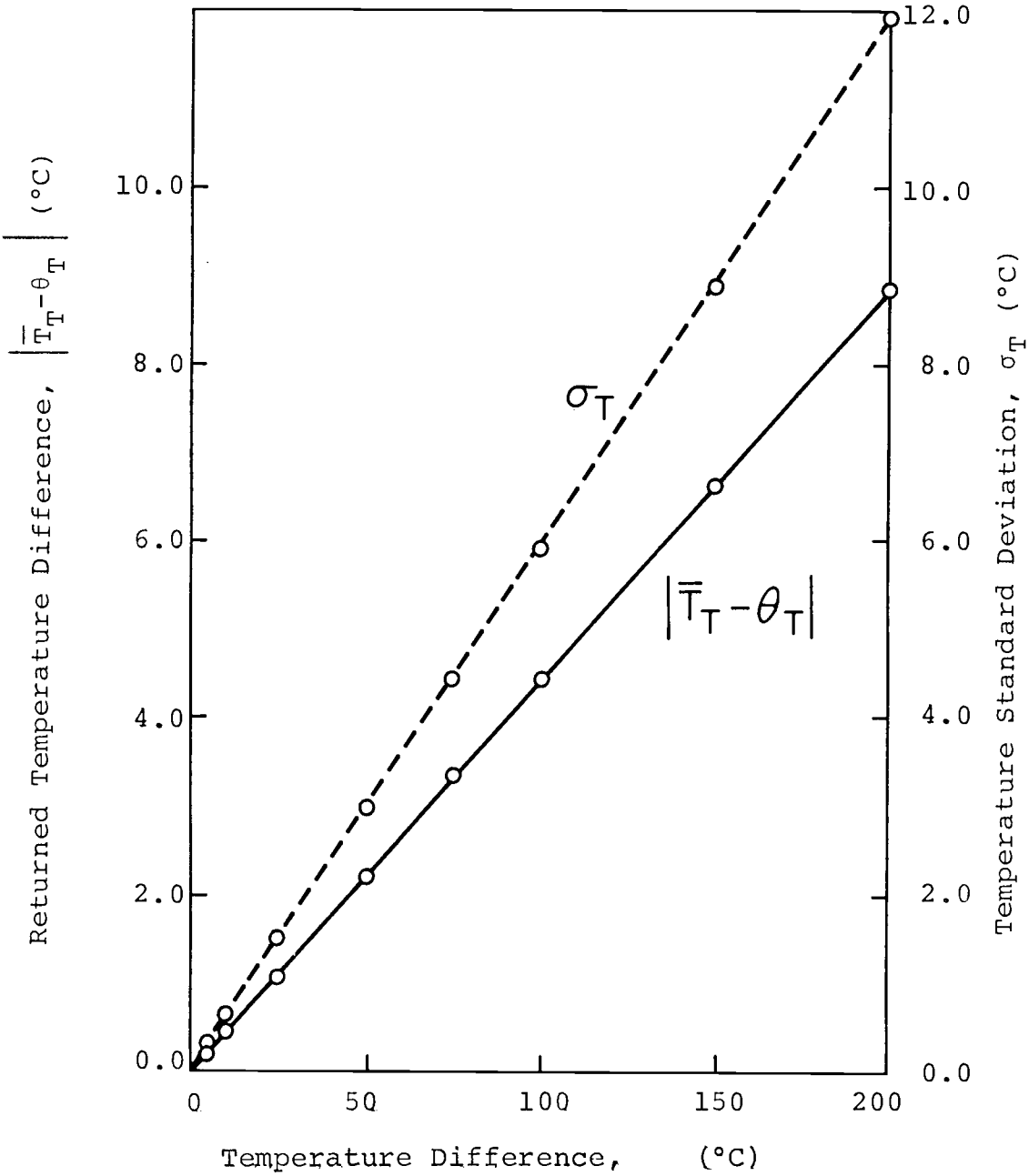

Figure 15: Returned accuracy versus temperature difference ($\Delta\theta$), $K_1<K_2$

conductivity is greater than the sphere conductivity, better accuracy is once again obtained. One unexpected observation was that the heat flux and its standard deviation remained constant for all values of $\Delta\theta$, if all other input parameters were constant. One note of interest, it was found, as would be expected, that the accuracy with which the boundary conditions were returned was not dependent upon whether the top face or the bottom face was at the higher temperature.

V. CONCLUSION

Completion of the analysis of the operating characteristics of the computer code shows that the basic goal has been achieved. Following the initial completion of the analytical solutions, computer coding of the solutions was begun. Development of the code was of assistance in determining errors in the analytical solutions. Secondly, as reasonable results were obtained, operation of the code provides confidence in the analytical expressions. And thirdly, limits have been determined on the accuracy of the code.

Because of the interrelation of the input parameters it becomes extremely difficult to place definite limits on what may, or may not, be used as input conditions. If it is desired, for example, to use $\Delta\theta = 50°C$, large deviations occur if $R_s/R_c = 1.0$ and $K_1/K_2 = 160.0$. However, if R_s/R_c were to be decreased and K_1/K_2 to approach one, then acceptable answers may be easily obtained. To further illustrate this a unit cell was considered with input conditions of $R_s/R_c = 0.5$, $K_2/K_1 = 10.0$ and $\Delta\theta = 5.0$. Table 10 tabulates

TABLE 10

RETURNED ACCURACY AND THE INTERRELATION

OF THE INPUT PARAMETERS

R_3 / R_c	k_2 / k_1	$\Delta\theta$ (°C)	$\lvert \bar{T}_T - \theta_T \rvert$ (°C)	σ_T (°C)	σ_ϕ (W/cm^2)
1.0	160	10	0.4421	0.5943	0.0759
0.5	160	10	0.0392	0.0493	0.0081
1.0	10	10	0.3650	0.4800	0.0600
1.0	160	5	0.2210	0.2972	0.0759
0.5	10	5	0.0112	0.0239	0.0071

the deviations that occur for a base unit cell of R_s/R_c = 10, K_2/K_1 = 160.0 and $\Delta\theta$ = 10.0, and the deviations that occur when each parameter is changed individually, and then finally the results from the above example where all three parameters are changed simultaneously.

From the data obtained in this investigation, it is concluded that the following limits should be followed. To use any value of R_s/R_c from 0 to 1 and any value of K_1/K_2 or K_2/K_1 from 1 to 160, the temperature difference should be maintained at less than ten degrees. If it is desired to use a larger temperature difference, then better answers will be obtained if the radius ratio can be reduced to less than 0.9, and/or if the conductivity ratio can be reduced to less than 25.0. It should always be kept in mind that the more homogeneous the unit cell, the better the accuracy which will be obtained.

Several general trends were observed in the overall temperature profiles of the unit cell. First, the temperature on the center plane, Z = 0, was a constant over the entire plane for all cases and was found to be $(\theta_T-\theta_B)/2$ within minor deviations. Secondly, the heat flux on the side face was symmetrical about the Z = 0 plane for all cases.

Thirdly, all temperatures within the unit cell were symmetrical about the Z = 0 plane for all cases. Fourth, as was expected, a sharp temperature change occurs in the lower conductivity material near the sphere-cell interface. The final observed trend was an unexpected result. It was expected that the region which would produce the greatest difficulty in obtaining accurate results would be the outer corner of the unit cell. This would be due to the difficulty of defining the cube in spherical geometry. After operation of the code, it was found that answers in this region did not deviate to any greater extent than any other region. However, for large differences in conductivity, and when the sphere has the larger conductivity, the calculated temperature for the point of intersection between the Z axis and the top face of the unit cell was significantly depressed relative to the input boundary condition and the average temperature on the top face of the unit cell.

There are some areas where further investigation is recommended and would be of interest. The first, and probably the most important, would be to allow for temperature dependent thermal conductivity. The analytical solution

could be modified to accept a variable conductivity rather than the present constant conductivity, but the computer code would be more difficult. An iterative process would most likely be the means to incorporate the variable conductivity into the computer code.

A second area of additional investigation which would be of value would be to study the effect of different sphere packing arrangements. These additional lattices could include a hexagonal two-dimensional packing and three dimensional lattices of the face-centered-cubic and body-centered cubic types. The only change in the analytical solution which these would require would be a change in the equations of the faces of the unit cell and subsequent changes in the derivations of the boundary conditions and limits of integration.

In summary, an analytical solution has been developed to solve for the temperature profile of a unit cell consisting of a sphere of one material centered in a cube of a second material. This was followed by the coding of a computer program using the analytical solution to calculate temperatures. From operation of the code it was concluded that the analytical solution was valid, and limits were

suggested to the input conditions to the code so as to maintain accurate results from the code.

BIBLIOGRAPHY

1) Schneider, G. E., "Thermal Resistance of a Cylinder With Two Diametrically Opposite, Symmetric, Isothermal Caps." Journal of Heat Transfer, August, 1975, pp. 465-7.

2) Yovanovich, M. Michael. Thermal Conductance of a Row of Cylinders Contacting Two Planes. Paper 71-346, AIAA 6th Thermophysics Conference, Tullahoma, Tenn., April 26-28, 1971.

3) Chan, C. K. and Tien, C. L. Conductance of Packed Spheres in Vacuum. Transactions of the ASME, August, 1975, p. 302-8.

4) Holy, Z. J. "Three Dimensional Temperature and Thermoelastic Stress Fields in a Heat Producing Sphere Due to Arbitrary Surface Heat Transfer." Nuclear Engineering and Design. 6 (1967), pp. 395-420.

5) Abramowitz, M. and Stegun, I. A., ed. Handbook of Mathematical Functions with Formulas, Graphs, and Mathematical Tables. National Bureau of Standards Applied Mathematics Series 55 (1965)

6) Prévost, Georges. Tables de Fonctions Sphériques. Paris: Gauthier-Villars et C^{ie}, Editeurs, p. 48.

7) Carnahan, B.; Luther, H. A.; Wilkes, J. O. Applied Numerical Methods. New York: J. Wiley & Sons, 1969. Problems 5.5 and 5.6, p. 330.

APPENDICES

Appendix A

Coordinate System Transformations and Unit Vectors

When deriving the equations for the unit cell faces, it is necessary to have the cartesian coordinate system (x, y, z) defined in terms of the spherical coordinate system (ρ, α, ϕ). From Figure A1 it is seen that ρ is the line from the origin to the point of interest. α is the angle between the z-axis and ρ. ϕ is the angle between the x axis and the projection of ρ on the x-y plane. The following relationships may be derived.

$$x = \rho\sin\alpha\cos\phi$$

$$y = \rho\sin\alpha\sin\phi$$

$$z = \rho\cos\alpha$$

The second necessary set of relationships is to define the spherical coordinate unit vectors in terms of the cartesian coordinate unit vectors. From Figure A1 these relationships may be derived as

$$\hat{e}_\rho = \sin\alpha\cos\phi\hat{e}_x + \sin\alpha\sin\phi\hat{e}_y + \cos\alpha\hat{e}_z$$

$$\hat{e}_\alpha = \cos\alpha\cos\phi\hat{e}_x + \cos\alpha\sin\phi\hat{e}_z - \sin\alpha\hat{e}_z$$

$$\hat{e}_\phi = -\sin\phi\hat{e}_x + \cos\phi\hat{e}_y$$

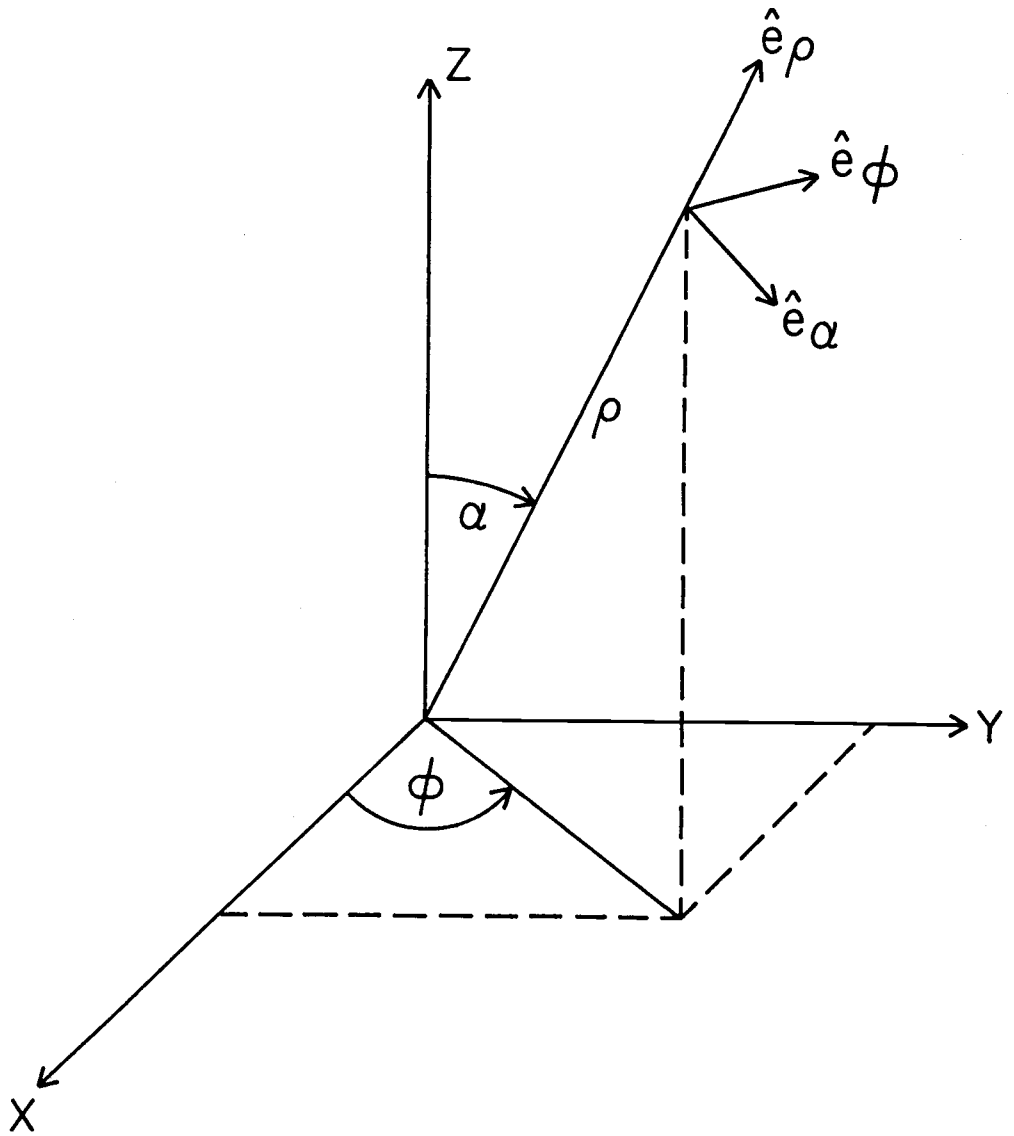

Figure A1: Coordinate system and spherical unit vectors

Appendix B

Derivation of the Limiting Conditions on μ

In defining the faces of the unit cell, it is necessary to define the limiting conditions for μ on each of the three faces, top, bottom and side. Figure B1 shows the upper half of the unit cell where point A is the midpoint of the sphere. Line ℓ_T is one of the limits to the top face of the unit cell. Line ℓ_T's unseen counterpart in the lower half of the unit cell (ℓ_B) defines one limit to the bottom face. Lines ℓ_T and ℓ_B also define two of the limits to the side face. The remaining defining limits to this face are $\phi = 0$ and $\phi = \pi/4$.

By observing the relationships pictured in Figure B1, it becomes possible to derive expressions for μ such that ρ (the line from point A to ℓ_T or ℓ_B) will intersect ℓ_T or ℓ_B.

Beginning with the three dimensional Pythagorean Theorem which states

$$a^2 + b^2 + c^2 = d^2$$

it can be seen from Figure B1 that the following holds.

$$\ell_1^2 + \ell_2^2 + \ell_3^2 = \rho^2 \qquad \text{(B-1)}$$

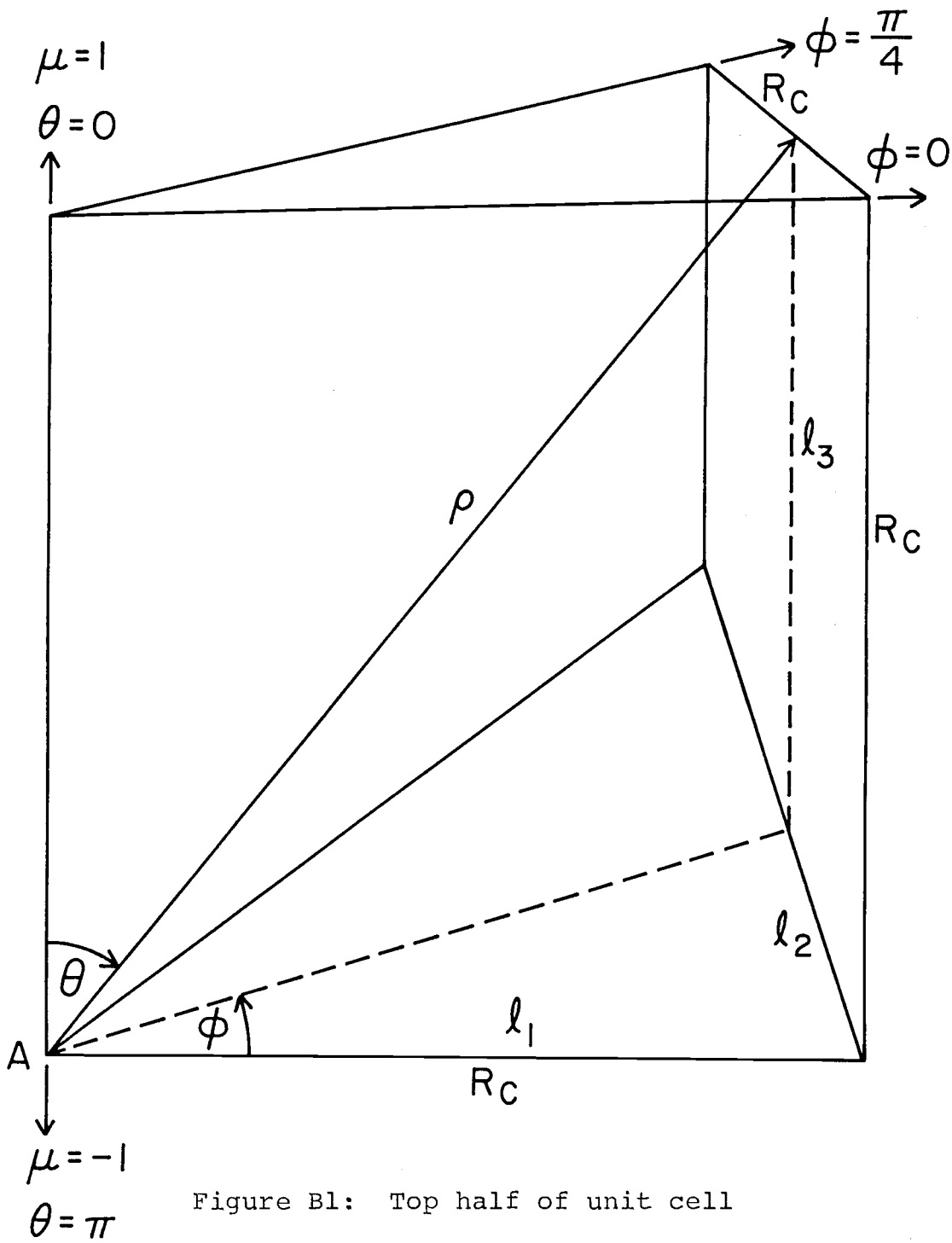

Figure B1: Top half of unit cell

Also from Figure B1 may be seen the following relationships.

$$\ell_1 = \ell_3 = R_c$$

$$\ell_3 = R_c = \rho\cos\theta$$

$$\ell_2 = \ell_1 \tan\phi = R_c \tan\phi$$

Now substituting in $R_c = \ell_1 = \ell_3$ into equation (B-1)

$$R_c^2 + \ell_2^2 + R_c^2 = \rho^2$$

$$2R_c^2 + \ell_2^2 = \rho^2$$

Next inserting the following expression for ρ

$$\rho = \frac{R_c}{\cos\theta}$$

and also the expression for ℓ_2, the following is obtained

$$2R_c^2 + R_c^2\tan^2\phi = \frac{R_c^2}{\cos\theta^2}$$

Now dividing through by R_c^2, inserting $\mu = \cos\theta$, and solving for μ

$$2 + \tan^2\phi = \frac{1}{\mu^2}$$

$$\mu = \frac{1}{(2+\tan^2\phi)^{1/2}} \qquad \text{(B-2)}$$

The corresponding equation which defines μ so that ρ intersects line ℓ_B is

$$\mu = \frac{-1}{(2+\tan^2\phi)^{1/2}} \qquad \text{(B-3)}$$

The limits on μ for all three faces may be written as

Top Face: $$\frac{1}{(2+\tan^2\phi)^{1/2}} \leq \mu \leq 1$$

Side Face: $$\frac{-1}{(2+\tan^2\phi)^{1/2}} \leq \mu \leq \frac{1}{(2+\tan^2\phi)^{1/2}}$$

Bottom Face: $$-1 \leq \mu \leq \frac{-1}{(2+\tan^2\phi)^{1/2}}$$

Appendix C

Equations of the Faces of the Unit Cell

To apply the boundary equations to the unit cell, it is necessary to define the faces of the unit cell in terms of ρ (the line from the center point of the sphere to any point on the face), and the limiting conditions on the face, μ and ϕ.

The two faces extending from the z axis are defined by $\phi = 0$ and $\phi = \pi/4$. The top and bottom faces and the opposing side face require more elaborate derivation. For these three faces the limiting conditions on ϕ and μ have already been determined (Appendix B). What remains is to derive expressions for ρ to each of the three faces. This may be done by using the equations in Appendix A which define the cartesian coordinates in terms of the spherical coordinates.

The top face of the unit cell is defined by $z = R_c$. The equation for this plane in spherical coordinates is

$$R_c = \rho\cos\theta$$

Solving for ρ and substituting in $\mu = \cos\theta$

$$\rho = R_c/\mu$$

Now non-dimensionalizing by the equation $r = \rho/R_c$

$$r = \frac{1}{\mu}$$

And this plane is bounded by

$$0 \leq \phi \leq \pi/4$$

$$\frac{1}{(2+\tan^2\phi)^{1/2}} \leq \mu \leq 1$$

The side face is defined by $x = R_c$. Solving for ρ

$$R_c = \rho\sin\theta\cos\phi$$

$$\rho = \frac{R_c}{\sin\theta\cos\phi}$$

Now substituting in $\sin\theta = (1-\mu^2)^{1/2}$ and non-dimensionalizing

$$r = \frac{1}{\cos\phi(1-\mu^2)^{1/2}}$$

The side face is bounded by

$$0 \leq \phi \leq \pi/4$$

$$\frac{-1}{(2+\tan^2\phi)^{1/2}} \leq \mu \leq \frac{1}{(2+\tan^2\phi)^{1/2}}$$

The bottom plane is defined by $z = R_c$. Using the same procedure as for the top face and solving for r

$$r = \frac{-1}{\mu}$$

The bottom face is bounded by

$$0 \leq \phi \leq \pi/4$$

$$-1 \leq \mu \leq \frac{-1}{(2+\tan^2\phi)^{1/2}}$$

Appendix D

Spherical Harmonic Expansion Coefficients

George Prévost (6) expands a function in terms of spherical harmonics in the following manner.

$$f(\mu,\alpha)=\sum_{n=0}^{\infty}\left[A_{n,0}\,P_{n,0}(\mu)+\sum_{j=0}^{j=n}\left(A_{nj}\cos(j\alpha)+B_{nj}\sin(j\alpha)\right)P_{nj}(\mu)\right]$$

where :

$$\mu = \cos\theta$$

$$0 \le \theta \le \pi$$

$$0 \le \alpha \le 2\pi$$

and:

$$A_{n,0} = \frac{2n+1}{4\pi}\int_0^{2\pi} d\alpha \int_{-1}^{1} f(\mu,\alpha)\,P_{n,0}(\mu)\,d\mu$$

$$B_{n,0} = 0$$

$$A_{nj} = \frac{2n+1}{2\pi}\,\frac{(n-j)!}{(n+j)!}\int_0^{2\pi} d\alpha \int_{-1}^{1} f(\mu,\alpha)\cos(j\alpha)\,P_{nj}(\mu)\,d\mu$$

$$B_{nj} = \frac{2n+1}{2\pi}\,\frac{(n-j)!}{(n+j)!}\int_0^{2\pi} d\alpha \int_{-1}^{1} f(\mu,\alpha)\sin(j\alpha)\,P_{nj}(\mu)\,d\mu$$

P_{nj} are the associated Legendre functions of the first kind.

Because of the symmetry of the unit cell, the B_{nj} terms are removed from further consideration. For the

unit cell under consideration, the functions $H(\mu,\phi)$ may be expanded as:

$$H(\mu,\phi) = A_{oo} + \sum_{\alpha=1}^{\infty}\sum_{\beta=0}^{(\alpha/4)} A_{\alpha\beta} P_{\alpha}^{4\beta}(\mu)\cos(4\beta\phi)$$

Prévost uses the condition $0 \leq \alpha \leq 2\pi$ to solve for the expansion coefficients. The unit cell under consideration is based upon the condition $0 \leq \phi \leq \pi/4$, therefore, making this change in integration and making appropriate changes in terminology, the expansion coefficients may be rewritten as:

$$A_{\alpha 0} = \frac{2(2\alpha+1)}{\pi}\int_0^{\pi/4} d\phi \int_{-1}^{1} H(\mu,\phi)\, P_{\alpha}(\mu)\, d\mu \qquad ,(\alpha = 0,n)$$

$$A_{\alpha\beta} = \frac{4(2\alpha+1)}{\pi}\,\frac{(\alpha-4\beta)!}{(\alpha+4\beta)!}\int_0^{\pi/4} d\phi \int_{-1}^{1} H(\mu,\phi)\, P_{\alpha}^{4\beta}(\mu)\cos(4\beta\phi)\, d\mu \qquad ,\begin{pmatrix}\alpha = 1,n \\ \beta = 0,\alpha/4\end{pmatrix}$$

To account for the change in the form of $H(\mu,\phi)$ with each of the three faces of the unit cell under consideration, the integral over μ may be broken into three integrals with the following form:

$$\int_{-1}^{1} d\mu = \int_{-1}^{A} d\mu + \int_{A}^{B} d\mu + \int_{B}^{1} d\mu$$

As shown in the main derivation, there are four $H(\mu,\phi)$ functions over the three faces of the unit cell. By inserting the appropriate functions, the expansion coefficients may now be written specifically.

$$A1_{\alpha 0} = \frac{2(2\alpha+1)}{\pi}\int_0^{\pi/4} d\phi \left(\int_{-1}^{-BC} P_\alpha(\mu)\, d\mu + \int_{BC}^{1} P_\alpha(\mu)\, d\mu \right)$$

$$A1_{\alpha\beta} = \frac{4(2\alpha+1)}{\pi}\,\frac{(\alpha-4\beta)!}{(\alpha+4\beta)!}\int_0^{\pi/4} d\phi \left(\int_{-1}^{-BC} P_\alpha^{4\beta}(\mu)\cos(4\beta\phi)\, d\mu \right.$$

$$\left. + \int_{BC}^{1} P_\alpha^{4\beta}(\mu)\cos(4\beta\phi)\, d\mu \right)$$

$$A2_{\alpha 0}^{nm} = \frac{2(2\alpha+1)}{\pi}\int_0^{\pi/4} d\phi \left(\int_{-1}^{-BC} \left(\frac{-1}{\mu}\right)^n P_n^{4m}(\mu)\cos(4m\phi)\, P_\alpha(\mu)\, d\mu \right.$$

$$+ \int_{-BC}^{BC} \left\{ \frac{\left(n P_n^{4m}(\mu) - (n+4m)\mu\, P_{n-1}^{4m}(\mu)\right)\cos(4m\phi)\cos\phi}{\cos^{n-1}\phi\,(1-\mu^2)^{n/2}} \right.$$

$$\left. \left. + \frac{4m\, P_n^{4m}(\mu)\sin(4m\phi)\sin\phi}{\cos^{n-1}\phi\,(1-\mu^2)^{n/2}} \right\} P_\alpha(\mu)\, d\mu \right.$$

$$\left. + \int_{BC}^{1} \left(\frac{1}{\mu}\right)^n P_n^{4m}(\mu)\cos(4m\phi)\, P_\alpha(\mu)\, d\mu \right)$$

$$A2_{\alpha\beta}^{nm} = \frac{4(2\alpha+1)}{\pi}\,\frac{(\alpha-4\beta)!}{(\alpha+4\beta)!}\int_0^{\pi/4} d\phi \left(\int_{-1}^{-BC} \left(\frac{-1}{\mu}\right)^n P_n^{4m}(\mu)\cos(4m\phi) \right.$$

$$\left. \cdot P_\alpha^{4\beta}(\mu)\cos(4\beta\phi)\, d\mu + \int_{-BC}^{BC} \left\{ \frac{\left(n P_n^{4m}(\mu) - (n+4m)\mu\, P_{n-1}^{4m}(\mu)\right)}{\cos^{n-1}\phi\,(1-\mu^2)^{n/2}} \right. \right.$$

$$\cdot \cos(4m\phi)\cos\phi + \frac{4m\, P_n^{4m}(\mu)\sin(4m\phi)\sin\phi}{\cos^{n-1}\phi\,(1-\mu^2)^{n/2}}\Bigg\}$$

$$\cdot P_\alpha^{4\beta}(\mu)\cos(4\beta\phi)\,d\mu + \int_{BC}^{1}\left(\frac{-1}{\mu}\right)^n P_n^{4m}(\mu)\cos(4m\phi)$$

$$\cdot P_\alpha^{4\beta}(\mu)\cos(4\beta\phi)\,d\mu\Bigg]$$

$$A3_{\alpha 0}^{nm} = \frac{2(2\alpha+1)}{\pi}\int_0^{\pi/4} d\phi\left[\int_{-1}^{-BC}\left(\frac{-1}{\mu}\right)^{-n-1} P_n^{4m}(\mu)\cos(4m\phi)\,P_\alpha(\mu)\,d\mu\right.$$

$$+\int_{-BC}^{BC}\left\{\frac{\left((\mu^2(2n+1)-(n+1)\right)P_n^{4m}(\mu)-(n+4m)\mu\,P_{n-1}^{4m}(\mu)\right)}{\cos^{-n-2}\phi\,(1-\mu^2)^{\frac{-n-1}{2}}}\right.$$

$$\left.\cdot\cos(4m\phi)\cos\phi + \frac{4m\,P_n^{4m}(\mu)\sin(4m\phi)\sin\phi}{\cos^{-n-2}\phi\,(1-\mu^2)^{\frac{-n-1}{2}}}\right\}P_\alpha(\mu)\,d\mu$$

$$\left.+\int_{BC}^{1}\left(\frac{1}{\mu}\right)^{-n-1} P_n^{4m}(\mu)\cos(4m\phi)\,P_\alpha(\mu)\,d\mu\right]$$

$$A3_{\alpha\beta}^{nm} = \frac{4(2\alpha+1)}{\pi}\frac{(\alpha-4\beta)!}{(\alpha+4\beta)!}\int_0^{\pi/4} d\phi\left[\int_{-1}^{-BC}\left(\frac{-1}{\mu}\right)^{-n-1} P_n^{4m}(\mu)\cos(4m\phi)\right.$$

$$\cdot P_\alpha^{4\beta}(\mu)\cos(4\beta\phi)\,d\mu + \int_{-BC}^{BC}\left\{\left(\mu^2(2n+1)-(n+1)\right)P_n^{4m}(\mu)\right.$$

$$\left.-(n+4m)\mu\,P_{n-1}^{4m}(\mu)\right)\frac{\cos(4m\phi)\cos\phi}{\cos^{-n-2}\phi\,(1-\mu^2)^{\frac{-n-1}{2}}}$$

$$+\left.\frac{4m\,P_n^{4m}(\mu)\sin(4m\phi)\sin\phi}{\cos^{-n-2}\phi\,(1-\mu^2)^{\frac{-n-1}{2}}}\right\} P_\alpha^{4\beta}(\mu)\cos(4\beta\phi)\,d\mu$$

$$\left.+\int_{BC}^{1}\left(\frac{1}{\mu}\right)^{-n-1} P_n^{4m}(\mu)\cos(4m\phi)\,P_\alpha^{4\beta}(\mu)\cos(4\beta\phi)\,d\mu\right)$$

$$A4_{\alpha 0} = \frac{2(2\alpha+1)}{\pi}\int_0^{\pi/4} d\phi \int_{BC}^{1} P_\alpha(\mu)\,d\mu$$

$$A4_{\alpha\beta} = \frac{4(2\alpha+1)}{\pi}\,\frac{(\alpha-4\beta)!}{(\alpha+4\beta)!}\int_0^{\pi/4} d\phi \int_{BC}^{1} P_\alpha^{4\beta}(\mu)\cos(4\beta\phi)\,d\mu$$

APPENDIX E

The Computer Code TEMPRO

The computer code TEMPRO was written based on the analytical derivation presented in this thesis. The code consists of the main program TEMPRO, two subroutines: ACALC and LINSOL, and four functions: GINTEG, P, FORIAL, and FCN. Input data consists of the thermal conductivities of the two materials (K_1, K_2), the sizes of the sphere and the cube (R_S, R_C), the temperature boundary conditions (θ_T, θ_B), the number of terms to be kept in the summation (n), and the number of points in the grid system for specifying where the temperatures are to be calculated (XPTS, YPTS, ZPTS). The output consists of a listing of all input data, the constants used in the final temperature solutions, the position of each grid point in cartesian and spherical coordinates, the temperature at each grid point and if that point is in the sphere or the surrounding cell, and the heat flux through the side face at all grid points on the side face of the unit cell.

The main program TEMPRO serves as the central coordinator and handles all input and output that is neces-

sary. TEMPRO begins by reading all input data, setting up output headers, and calculating the limits and points of integration. Once all necessary data is developed, TEMPRO calls subroutine ACALC which calculates the spherical harmonic expansion coefficients. TEMPRO then places the coefficients into a system of linear equations as defined by equation (III-32). Subroutine LINSOL solves the matrix and returns the coefficients $C_{oo}^{(1)}$ and $C_{nm}^{(1)}$. The next step in TEMPRO is to solve for $C_{oo}^{(2)}$, $C_{nm}^{(2)}$ and $C_{nm}^{(3)}$ from $C_{oo}^{(1)}$ and $C_{nm}^{(1)}$. All constants are now known and it is possible to solve for the temperature at any point within the unit cell. TEMPRO automatically steps through a grid system defined by XPTS, YPTS, and ZPTS and calculates the temperature at all grid points. The cartesian coordinate system is used for input and output because of its ease of use and easier visualization. All work within the body of TEMPRO is performed in the spherical coordinate system. Similarly, the size of the cube and the sphere, and the temperature boundary conditions, are read in and out in absolute units (cm and °C), and then internally converted with TEMPRO to non-dimensional quantities.

Subroutine ACALC and function GINTEG work to-

gether to calculate the spherical harmonic expansion coefficients that are defined in Appendix D. ACALC begins by setting up the proper expressions to calculate the expansion coefficients. This is done by calculating the necessary factor to multiply each integral by, and then defines the integral limits, function, and face of the unit cell which is to be integrated. GINTEG uses this information to calculate the desired integral. For the integration GINTEG uses a 10-point, two-dimensional Gauss-Legendre Quadrature system which was specifically derived for the unit cell under consideration in this thesis.

The associated Legendre functions and the expressions used to calculate the expansion coefficients are found in the functions P and FCN respectively. P contains the analytical expressions for all associated Legendre functions that are necessary for the temperature solutions. Input parameters consist of n, 4m and μ, and the numerical evaluation is returned. FCN is a listing of the expressions found in the analytical expressions for the expansion coefficients. It is entered with FNUM requesting a specific expression within the function, and then that expression is evaluated for the parameters μ, ϕ, γ, η, n and 4m. This

value is then returned to GINTEG.

Subroutine LINSOL uses the Gauss-Jordan method of linear equation solving to solve the system of linear equations defined by equation (III-32). To improve the accuracy of the values of $C_{oo}^{(1)}$ and $C_{nm}^{(1)}$ returned by LINSOL, the subroutine uses an iterative improvement procedure as outlined by Carnahan (7).

```
      PROGRAM TEMPRO(INPUT,OUTPUT,TAPE20)
      COMMON/1/ A(18,19),A1(10,3),A2(10,3,17),A3(10,3,17)
     ^,A4(10,3),C(10,3,3),FOUR
      COMMON/2/G(3,10,10),WEIGHT(10),ALIM(30),BLIM(30),
     ^PHI(10)
      DIMENSION ROOT(10)
      REAL K1,K2,M4
      INTEGER GAMMA,AETA
      DATA(ROOT=.1488743389,-.1488743389,.4333953941,
     ^-.4333953941,.6794095682,-.6794095682,.8650633666,
     ^-.8650633666,.9739065285,-.9739065285)
      DATA(WEIGHT=.2955242247,.2955242247,.2692667193,
     ^.2692667193,.2190863625,.2190863625,.1494513491,
     ^.1494513491,.06667134430,.0666713443)
      DATA(PI=3.141592654)
C
C          SET UP HEADERS AND LIMITS OF INTEGRATION
C
      GO TO 1100
 1000 PRINT*,'IF NO NEW DATA, TYPE 1'
      READ*,INDATA
      IF(INDATA.EQ.1)GO TO 1200
 1100 PRINT*,'INPUT SPHERE K, CELL K'
      READ*,K1,K2
      PRINT*,'INPUT SPHERE R, CELL R'
      READ*,RSPHERE,RCUBE
      RATIO=RSPHERE/RCUBE
      PRINT*,'INPUT TOP TEMP, BOTTOM TEMP'
      READ*,TTEMP,BTEMP
      FOUR=4.
 1200 PRINT(20,*)' '
      PRINT(20,*)'SPHERE RADIUS= ',RSPHERE,' CM'
      PRINT(20,*)'CUBE RADIUS= ',RCUBE,' CM'
      PRINT(20,*)'SPHERE CONDUCTIVITY= ',K1,' WATTS/CM C'
      PRINT(20,*)'CELL CONDUCTIVITY= ',K2,' WATTS/CM C'
      PRINT(20,*)'TOP TEMP PROFILE= ',TTEMP,' DEGREES C'
      PRINT(20,*)'BOTTOM TEMP PROFILE= ',BTEMP,' DEGREES C'
      PRINT*,'THIS PROGRAM WILL ACCEPT UP TO 9 TERMS'
      PRINT*,'INPUT NUMBER OF TERMS'
      READ*,NTERM
      PRINT(20,*)'FOR THIS RUN, THE NUMBER OF TERMS= ',NTERM
      DO 300 I=1,10
      PHI(I)=(ROOT(I)+1.)*PI/8.
      ALIM(I)=-1.
  300 BLIM(I)=-1./SQRT(2.+TAN(PHI(I))**2)
      DO 302 I=11,20
      ALIM(I)=BLIM(I-10)
  302 BLIM(I)=-ALIM(I)
```

```
      DO 303 I=21,30
      ALIM(I)=BLIM(I-10)
  303 ELIM(I)=1.
C
C        IBC=1, BOTTOM FACE
C        IBC=2, SIDE FACE
C        IBC=3, TOP FACE
C
      DO 1300 IBC=1,3
      IF(IBC.EQ.1)L=0
      IF(IBC.EQ.2)L=10
      IF(IBC.EQ.3)L=20
      DO 1400 J=1,10
      DO 1400 I=1,10
      G(IBC,J,I)=(ROOT(I)*(BLIM(J+L)-ALIM(J+L))+BLIM(J+L)+
     ^ALIM(J+L))/2.
 1400 CONTINUE
 1300 CONTINUE
      IF(NTERM.LE.3)MS=NTERM+1
      IF(4.LE.NTERM .AND. NTERM.LE.7)MS=2*NTERM-2
      IF(8.LE.NTERM .AND. NTERM.LE.11)MS=3*NTERM-9
      MS1=MS+1
C
C           CALCULATE A1,A2,A3,A4
C
      CALL ACALC(NTERM)
      M1=NTERM+1
C
C           SET UP 'A' MATRIX FOR SOLUTION
C
      I=1
      DO 801 GAMMA=1,M1
      IF(GAMMA.LE.4)J=1
      IF(5.LE.GAMMA .AND. GAMMA.LE.8)J=2
      IF(9.LE.GAMMA .AND. GAMMA.LE.12)J=3
        DO 803 AETA=1,J
      MM=1
        A(I,1)=A1(GAMMA,AETA)
        A(I,MS1)=A4(GAMMA,AETA)
        I2=2
          DO 811 NN=1,NTERM
          IF(NN.LE.3)K=1
          IF(4.LE.NN .AND. NN.LE.7)K=2
          IF(8.LE.NN .AND. NN.LE.11)K=3
            DO 813 MM=1,K
            A(I,I2)=A2(GAMMA,AETA,MM)*(K2*(NN+1.)+K1*NN)
     ^      /(K2*(2.*NN+1.))+A3(GAMMA,AETA,MM)*(1.-K1/K2)*
     ^      RATIO**(2*NN+1)*NN/(2.*NN+1.)
```

```
            NM=NM+1
            I2=I2+1
  813       CONTINUE
  811     CONTINUE
        I=I+1
  803   CONTINUE
  801 CONTINUE
C
C          SOLVE 'A' MATRIX
C
      CALL LINSOL(MS,MS1)
C
C          SET UP CONSTANTS 'C'
C
      I=2
      DO 20 NN=2,N1
      NN1=NN-1
      IF(NN.LE.4)K=1
      IF(5.LE.NN .AND. NN.LE.8)K=2
      IF(9.LE.NN .AND. NN.LE.12)K=3
        DO 22 MM=1,K
        C(NN,MM,1)=A(I,MS1)
        C(NN,MM,2)=C(NN,MM,1)*(K2*NN+K1*NN1)/(K2*(2.*NN1+1.))
        C(NN,MM,3)=C(NN,MM,1)*(1.-K1/K2)*RATIO**(2*NN1+1)*NN1
     *  /(2.*NN1+1.)
        I=I+1
   22   CONTINUE
   20 CONTINUE
      C(1,1,1)=C(1,1,2)=A(1,MS1)
      PRINT(20,69)
   69 FORMAT(1X,'C VALUES'/17X,'CNM1',9X,'CNM2',9X,'CNM3')
      DO 860 I=1,N1
      IF(I.LE.4)K=1
      IF(5.LE.I .AND. I.LE.8)K=2
      IF(9.LE.I .AND. I.LE.12)K=3
      DO 861 J=1,K
      PRINT(20,862)I,J,C(I,J,1),C(I,J,2),C(I,J,3)
  862 FORMAT(1X,'N=',I2,2X,'M=',I2,3(2X,E11.5))
  861 CONTINUE
  860 CONTINUE
C
C        AUTOMATIC STEP THROUGH OF UNIT CELL AND
C            CALCULATION OF TEMPERATURES AT ALL
C            POINTS AND HEAT FLUXES ON SURFACES
C            OF UNIT CELL
C
      PRINT(20,100)
  100 FORMAT(1X/30X,'POSITION',35X,'TEMPERATURE',10X,'HEAT'
```

```
     ^,≠ FLUX≠)
      PRINT(20,101)
101  FORMAT(4X,≠X≠,10X,≠Y≠,10X,≠Z≠,10X,≠R≠,10X,≠MU≠,10X,
     ^≠FEE≠,8X,≠SPHERE≠,7X,≠CELL≠,8X,≠SIDE≠)
      PRINT*,≠INPUT XPTS, YPTS, ZPTS≠
      READ*,XPTS,YPTS,ZPTS
      XH=1./(XPTS-1.)
      YH=1./(YPTS-1.)
      ZH=2./(ZPTS-1.)
      X=Y=0
      XT=YT=0
      Z=1.
      ZT=RCUBE
      GO TO 200
201   X=X+XH
      XT=X*RCUBE
      IF(X.GT.1.)GO TO 202
      GO TO 200
202   Y=Y+YH
      YT=Y*RCUBE
      IF(Y.GT.1.)GO TO 203
      X=0
      GO TO 200
203   Z=Z-ZH
      PRINT(20,*)≠ ≠
      ZT=Z*RCUBE
      IF(Z.LT.-1.)GO TO 600
      X=Y=0
      XT=YT=0
200   XR=SQRT(X*X+Y*Y+Z*Z)
      XRT=XR*RCUBE
      IF(Z.EQ.0)GO TO 205
      THETA=ACOS(Z/XR)
      XMU=COS(THETA)
      IF(XMU.EQ.1)XMU=.9999
      IF(XMU.EQ.-1)XMU=-.9999
      IF(Y.EQ.0)GO TO 206
      XFEE=ATAN(Y/X)
      IF(XFEE.GT..7854)GO TO 201
      IF(XR.GT.RATIO)GO TO 3
      GO TO 210
205   XMU=.0001
      IF(X.EQ.0 .AND. Y.NE.0)GO TO 201
      IF(Y.EQ.0)XFEE=0
      IF(Y.NE.0)XFEE=ATAN(Y/X)
      IF(XFEE.GT..7854)GO TO 201
      IF(XR.GT.RATIO)GO TO 3
      GO TO 210
```

```
  206 XFEE=0
      IF(XR.GT.RATIO)GO TO 3
C
C           CALCULATION OF TEMPERATURE WITHIN SPHERE
C
  210 TEMP1=0
      DO 40 NN=2,N1
      IF(NN.LE.4)K=1
      IF(5.LE.NN .AND. NN.LE.8)K=2
      IF(9.LE.NN .AND. NN.LE.12)K=3
        DO 42 MM=1,K
        M4=(MM-1.)*FOUR
        TEMP1=TEMP1+C(NN,MM,1)*XR**(NN-1)*P(NN,MM,XMU)*
     ^  COS(M4*XFEE)
   42   CONTINUE
   40 CONTINUE
      TEMP1=(TEMP1+C(1,1,1))*(TTEMP-BTEMP)+BTEMP
      IF(XR.EQ.0)GO TO 6900
      IF(XR.EQ.RATIO)GO TO 3
 6900 PRINT(20,103)XT,YT,ZT,XRT,XMU,XFEE,TEMP1
  103 FORMAT(1X,6(F8.4,3X),F10.4)
      GO TO 201
C
C           CALCULATION OF TEMPERATURE OUTSIDE OF SPHERE
C
    3 TEMP2=0
      DO 43 NN=2,N1
      IF(NN.LE.4)K=1
      IF(5.LE.NN .AND. NN.LE.8)K=2
      IF(9.LE.NN .AND. NN.LE.12)K=3
        DO 45 MM=1,K
        M4=(MM-1.)*FOUR
        TEMP2=TEMP2+(C(NN,MM,2)*XR**(NN-1)+C(NN,MM,3)*XR**
     ^  (-NN))*P(NN,MM,XMU)*COS(M4*XFEE)
   45   CONTINUE
   43 CONTINUE
      TEMP2=(TEMP2+C(1,1,2))*(TTEMP-BTEMP)+BTEMP
      IF(X.GE.1.)GO TO 500
      IF(XR.EQ.RATIO)GO TO 502
      PRINT(20,104)XT,YT,ZT,XRT,XMU,XFEE,TEMP2
  104 FORMAT(1X,6(F8.4,3X),11X,F10.4)
      GO TO 201
  502 PRINT(20,105)XT,YT,ZT,XRT,XMU,XFEE,TEMP1,TEMP2
  105 FORMAT(1X,6(F8.4,3X),2(F10.4,3X))
      GO TO 201
C
C           CALCULATION OF HEAT FLUX ON SIDE FACE
C
```

```
500  FLUX=0
     DO 91 NN=2,N1
     NN1=NN-1
     IF(NN.LE.4)K=1
     IF(5.LE.NN .AND. NN.LE.8)K=2
     IF(9.LE.NN .AND. NN.LE.12)K=3
       DO 93 MM=1,K
       M4=(MM-1.)*FOUR
       FLUX=FLUX+C(NN,MM,2)/COS(XFEE)**(NN1-1)
    &  /(1.-XMU*XMU)**(NN1/2.)*(COS(M4*XFEE)*COS(XFEE)*
    &  (NN1*P(NN,MM,XMU)-(NN1
    &  +M4)*XMU*P(NN1,MM,XMU))+M4*P(NN,MM,XMU)*SIN(M4*XFEE)
    &  *SIN(XFEE))+C(NN,MM,3)/COS(XFEE)**(-NN1-2)
    &  /(1.-XMU*XMU)**((-NN1-1.)/2.)*(COS(M4*XFEE)*COS(XFEE)*
    &  ((XMU*XMU*(2.*NN1+1.)-NN)*P(NN,MM,XMU)-(NN1+M4)*
    &  XMU*P(NN1,MM,XMU))+M4*P(NN,MM,XMU)*SIN(M4*XFEE)*
    ^  SIN(XFEE))
 93    CONTINUE
 91  CONTINUE
     PRINT(20,107)XT,YT,ZT,XRT,XMU,XFEE,TEMP2,FLUX
107  FORMAT(1X,6(F8.4,3X),11X,2(F10.4,3X))
     GO TO 201
600  PRINT*,≠IF WANT TO CONTINUE, TYPE 1≠
     READ*,CONT
     IF(CONT.EQ.1)GO TO 1000
     STOP
     END
ƒ
6

     SUBROUTINE ACALC(NTERM)
     COMMON/1/ A(18,19),A1(10,3),A2(10,3,17),A3(10,3,17)
    ^,A4(10,3),C(10,3,3),FOUR
     INTEGER GAMMA,AETA,G1
     DATA(PI=3.141592654)
     N1=NTERM+1
     DO 1 GAMMA=1,N1
     IF(GAMMA.LE.4)J=1
     IF(5.LE.GAMMA .AND. GAMMA.LE.8)J=2
     IF(9.LE.GAMMA .AND. GAMMA.LE.12)J=3
       DO 3 AETA=1,J
     MM=1
       G1=GAMMA-1
       L1=G1-FOUR*(AETA-1)
       L2=G1+FOUR*(AETA-1)
       FACTOR=(2*G1+1)*4./PI*FORIAL(L1)/FORIAL(L2)
       IF(AETA.EQ.1)FACTOR=FACTOR/2.
       A1(GAMMA,AETA)=FACTOR*(GINTEG(1,1,GAMMA,AETA,0,0)
    &  +GINTEG(3,1,GAMMA,AETA,0,0))
```

```
      A4(GAMMA,AETA)=FACTOR*GINTEG(3,1,GAMMA,AETA,0,0)
        DO 4 NN=1,NTERM
        IF(NN.LE.3)K=1
        IF(4.LE.NN .AND. NN.LE.7)K=2
        IF(8.LE.NN .AND. NN.LE.11)K=3
          DO 6 MM=1,K
          A2(GAMMA,AETA,NM)=FACTOR*(GINTEG(1,2,GAMMA,
     ^    AETA,NN,MM)+GINTEG(2,3,GAMMA,AETA,NN,MM)+
     ^    GINTEG(3,4,GAMMA,AETA,NN,MM))
          A3(GAMMA,AETA,NM)=FACTOR*(GINTEG(1,5,GAMMA,
     ^    AETA,NN,MM)+GINTEG(2,6,GAMMA,AETA,NN,MM)+
     ^    GINTEG(3,7,GAMMA,AETA,NN,MM))
          NM=NM+1
    6     CONTINUE
    4   CONTINUE
    3 CONTINUE
    1 CONTINUE
      RETURN
      END
C
C
      FUNCTION GINTEG(BC,FNUM,GAMMA,AETA,NN,MM)
      COMMON/2/G(3,10,10),WEIGHT(10),ALIM(30),BLIM(30),
     ^PHI(10)
      DIMENSION Z(10)
      INTEGER BC,FNUM,GAMMA,AETA
      DATA(PI=3.141592654)
      SUM1=0
      IF(BC.EQ.1)L=0
      IF(BC.EQ.2)L=10
      IF(BC.EQ.3)L=20
      DO 9 J=1,10
      SUM=0
        DO 10 I=1,10
   10   SUM=SUM+WEIGHT(I)*FCN(G(BC,J,I),PHI(J),FNUM,GAMMA,
     ^  AETA,NN,MM)
      Z(J)=(BLIM(L+J)-ALIM(L+J))/2.*SUM
    9 CONTINUE
      DO 11 I=1,10
   11 SUM1=SUM1+WEIGHT(I)*Z(I)
      GINTEG=PI/8.*SUM1
      RETURN
      END
C
C
      FUNCTION P(N,M,MU)
      REAL MU,MU2
      MU2=MU*MU
```

```
      GO TO(10,20,30,40,50,60,70,80,90,100,110)N
   10 P=1
      RETURN
   20 P=MU
      RETURN
   30 P=(3*MU2-1)/2
      RETURN
   40 GO TO(41,42)M
   41 P=((5*MU2-3)*MU)/2
      RETURN
   42 P=0
      RETURN
   50 GO TO(51,52)M
   51 P=((35*MU2-30)*MU2+3)/8
      RETURN
   52 P=105*(1-MU2)**2
      RETURN
   60 GO TO(61,62)M
   61 P=(((63*MU2-70)*MU2+15)*MU)/8
      RETURN
   62 P=945*MU*(1-MU2)**2
      RETURN
   70 GO TO(71,72)M
   71 P=(((231*MU2-315)*MU2+105)*MU2-5)/16
      RETURN
   72 P=945/2*(1-MU2)**2*(11*MU2-2)
      RETURN
   80 GO TO(81,82,83)M
   81 P=((((429*MU2-693)*MU2+315)*MU2-35)*MU)/16
      RETURN
   82 P=3465/2*(1-MU2)**2*((13*MU2-3)*MU)
      RETURN
   83 P=0
      RETURN
   90 GO TO(91,92,93)M
   91 P=((((6435*MU2-12012)*MU2+6930)*MU2-1260)*MU2+35)/128
      RETURN
   92 P=10395/8*(1-MU2)**2*((65*MU2-26)*MU2+1)
      RETURN
   93 P=2027025*(1-MU2)**4
      RETURN
  100 GO TO(101,102,103)M
  101 P=((((12155*MU2-25740)*MU2+18018)*MU2-4620)*MU2
     *+315)*MU)/128
      RETURN
  102 P=1351 35/8*(1-MU2)**2*(((17*MU2-10)*MU2+1)*MU)
      RETURN
  103 P=34459425*MU*(1-MU2)**4
```

```
      RETURN
  110 GO TO(111,112,113)M
  111 P=((((46189*MU2-109395)*MU2+90090)*MU2-30030)*MU2
     ↱+3465)*MU2-63)/256
      RETURN
  112 P=45045/16*(1-MU2)**2*(((323*MU2-255)*MU2+45)*MU2-1)
      RETURN
  113 P=34459425/2*(19*MU2-1)*(1-MU2)**4
      RETURN
      END
$
$
      FUNCTION FCN(MU,FEE,FNUM,GAMMA,AETA,N,M)
      COMMON/1/ A(18,19),A1(10,3),A2(10,3,17),A3(10,3,17)
     ^,A4(10,3),C(10,3,3),FOUR
      REAL MU,M4
      INTEGER FNUM,GAMMA,AETA,AETA4
      N1=N+1
      AETA4=(AETA-1)*FOUR
      M4=(M-1.)*FOUR
      IF(M.EQ.0)M4=0
      GO TO (1,2,3,4,5,6,7)FNUM
    1 FCN=P(GAMMA,AETA,MU)*COS(AETA4*FEE)
      RETURN
    2 FCN=(-1./MU)**N*P(N1,M,MU)*COS(M4*FEE)*
     ↱P(GAMMA,AETA,MU)*COS(AETA4*FEE)
      RETURN
    3 FCN=(1./COS(FEE)**(N-1)/(1.-MU*MU)**(N/2.)
     ↱*((N*P(N1,M,MU)-(N+M4)*MU*P(N,M,MU))*COS(M4*FEE)
     ↱*COS(FEE)+M4*P(N1,M,MU)*SIN(M4*FEE)*SIN(FEE)))
     ↱*P(GAMMA,AETA,MU)*COS(AETA4*FEE)
      RETURN
    4 FCN=(1./MU)**N*P(N1,M,MU)*COS(M4*FEE)*P(GAMMA,AETA,
     ↱MU)*COS(AETA4*FEE)
      RETURN
    5 FCN=(-1./MU)**(-N-1)*P(N1,M,MU)*COS(M4*FEE)*P(GAMMA,
     ↱AETA,MU)*COS(AETA4*FEE)
      RETURN
    6 FCN=(1./COS(FEE)**(-N-2)/(1.-MU*MU)**((-N-1.)/2.)
     ^*(((MU*MU*(2.*N+1.)-N1)*P(N1,M,MU)-(N+M4)*MU*
     ^P(N,M,MU))*COS(M4*FEE)*COS(FEE)+M4*P(N1,M,MU)*
     ^SIN(M4*FEE)*SIN(FEE)))*P(GAMMA,AETA,MU)
     ^*COS(AETA4*FEE)
      RETURN
    7 FCN=(1./MU)**(-N-1)*P(N1,M,MU)*COS(M4*FEE)*
     ↱P(GAMMA,AETA,MU)*COS(AETA4*FEE)
      RETURN
      END
```

```
$
$
      SUBROUTINE LINSOL(N,NP)
      COMMON/1/ A(18,19),A1(10,3),A2(10,3,17),A3(10,3,17)
     ^,A4(10,3),C(10,3,3),FOUR
      DIMENSION D(20,21),E(20,40),X(20),
     *P(20),DELB(20),DELX(20),AX(20)
      ATEMP=0.
      DO 9 I=1,N
        DO 8 J=1,N
        TEMP=ABS(A(I,J))
        IF(TEMP.GE.ATEMP)ATEMP=TEMP
    8   CONTINUE
          DO 10 J=1,NP
   10     D(I,J)=A(I,J)/ATEMP
    9 CONTINUE
      DO 3 K=1,N
      KP=K+1
      ATEMP=0.
      L=K
        DO 4 I=K,N
        TEMP=ABS(D(I,K))
        IF(TEMP-ATEMP)4,4,5
    5   L=I
        ATEMP=TEMP
    4   CONTINUE
      IF(L-K)6,28,6
    6   DO 7 J=K,NP
        TEMP=D(L,J)
        D(L,J)=D(K,J)
    7   D(K,J)=TEMP
   28 CONTINUE
        DO 3 J=KP,NP
        D(K,J)=D(K,J)/D(K,K)
          DO 3 I=1,N
          IF(I.EQ.K)GO TO 3
          D(I,J)=D(I,J)-D(K,J)*D(I,K)
    3   CONTINUE
      N2=2*N
      DO 70 I=1,N
      DO 70 J=1,N
   70 E(I,J)=A(I,J)
      DO 32 I=1,N
      DO 32 J=NP,N2
      IF(I+N.EQ.J)GO TO 31
      E(I,J)=0.
      GO TO 32
   31 E(I,J)=1.
```

```
32 CONTINUE
   ATEMP=0.
   DO 1 I=1,N
     DO 2 J=1,N
     TEMP=ABS(E(I,J))
     IF(TEMP.GE.ATEMP)ATEMP=TEMP
 2   CONTINUE
       DO 11 J=1,N2
11     E(I,J)=E(I,J)/ATEMP
 1 CONTINUE
   DO 13 K=1,N
   KP=K+1
   ATEMP=0
   L=K
     DO 14 I=K,N
     TEMP=ABS(E(I,K))
     IF(TEMP-ATEMP)14,14,15
15   L=I
     ATEMP=TEMP
14   CONTINUE
     IF(L-K)16,18,16
16   DO 17 J=K,N2
     TEMP=E(L,J)
     E(L,J)=E(K,J)
17   E(K,J)=TEMP
18   CONTINUE
     DO 13 J=KP,N2
     E(K,J)=E(K,J)/E(K,K)
       DO 13 I=1,N
       IF(I.EQ.K)GO TO 13
       E(I,J)=E(I,J)-E(K,J)*E(I,K)
13   CONTINUE
   DO 21 I=1,N
   X(I)=D(I,NP)
21 B(I)=A(I,NP)
   SUM=0
   DO 25 I=1,N
     DO 26 J=1,N
26   SUM=SUM+A(I,J)*X(J)
   AX(I)=SUM
25 SUM=0
   DO 22 I=1,N
22 DELB(I)=B(I)-AX(I)
   SUM=0
   DO 23 I=1,N
     DO 29 J=NP,N2
29   SUM=SUM+E(I,J)*DELB(J-N)
   DELX(I)=SUM
```

```
   23 SUM=0
      DO 24 I=1,N
      A(I,NP1)=DELX(I)+X(I)
   24 CONTINUE
      RETURN
      END
C
C
      FUNCTION FORIAL(J)
      FORIAL=1
      DO 1 I=1,J
    1 FORTAL=FORIAL*I
      RETURN
      END
```

APPENDIX F

Reduction of the Three Dimensional Solution to Two Dimensions

Under some circumstances it may be desirable to reduce the three dimensional temperature solution, that has been presented here, to a two dimensional solution. This solution may be obtained by removing all dependence upon ϕ. The resulting unit cell will appear as in Figure 5b and will be representative of a sphere centered within a cylinder and thus having no ϕ dependence.

All boundary conditions will remain the same and the two dimensional solution will be obtained by evaluating all equations at $\phi = 0$. For $\phi = 0$ it then follows that $m = 0$ and this has two effects. First, it removes the summation over m, and secondly, it causes a change from associated Legendre polynomials to special Legendre polynomials. That is because by definition (5), $P_n^0(\mu) = P_n(\mu)$.

The primary equations reduce to the following equations for a two dimensional analysis.

Temperature Solutions:

$$T_1(r,\mu,\phi) = C_o^{(1)} + \sum_{n=1}^{\infty} C_n^{(1)} r^n P_n(\mu)$$

$$T_2(r,\mu,\phi) = C_o^{(2)} + \sum_{n=1}^{\infty} \left(C_n^{(2)} r^n + C_n^{(3)} r^{-n-1} \right) P_n(\mu)$$

Top Face Boundary Condition:

$$r = \frac{1}{\mu}$$

$$\frac{1}{\sqrt{2}} \leq \mu \leq 1$$

$$1 = C_o^{(2)} + \sum_{n=1}^{\infty} \left[C_n^{(2)} \left(\frac{1}{\mu}\right)^n P_n(\mu) + C_n^{(3)} \left(\frac{1}{\mu}\right)^{-n-1} P_n(\mu) \right]$$

Side Face Boundary Condition:

$$r = \frac{1}{(1-\mu^2)^{1/2}}$$

$$\frac{-1}{\sqrt{2}} \leq \mu \leq \frac{1}{\sqrt{2}}$$

$$0 = \sum_{n=1}^{\infty} \left\{ \frac{C_n^{(2)}}{(1-\mu^2)^{n/2}} \left[n P_n(\mu) - n P_{n-1}(\mu) \right] + \frac{C_n^{(3)}}{(1-\mu^2)^{\frac{-n-1}{2}}} \right.$$

$$\left. \cdot \left[\left((1\mu^2(2n+1) - (n+1) \right) P_n(\mu) - n\mu P_{n-1}(\mu) \right) \right] \right\}$$

Bottom Face Boundary Condition:

$$r = \frac{-1}{\mu}$$

$$-1 \leq \mu \leq \frac{-1}{\sqrt{2}}$$

$$0 = C_o^{(2)} + \sum_{n=1}^{\infty} \left[C_n^{(2)} \left(\frac{-1}{\mu}\right)^n P_n(\mu) + C_n^{(3)} \left(\frac{-1}{\mu}\right)^{-n-1} P_n(\mu) \right]$$

System of Linear Equations:

$$A1_\gamma C_o^{(1)} + \sum_{n=1}^{\infty} \left\{ C_n^{(1)} \left[A2_\gamma^n \left(\frac{K_2(n+1) + K_1 n}{K_2(2n+1)} \right) + A3_\gamma^n \frac{(1 - K_1/K_2) n R_a^{2n+1}}{2n+1} \right] \right\} = A4_\gamma$$

$$\left(R_a = \frac{R_3}{R_c} \right)$$